

Temporal and Hf isotope geochemical evolution of southern Finnish Lapland from 2.77 Ga to 1.76 Ga

L.S. LAURI^{1)*}, T. ANDERSEN²⁾, J. RÄSÄNEN¹⁾ AND H. JUOPPERI¹⁾



¹⁾ Geological Survey of Finland, P.O. Box 77, FI-96101 Rovaniemi, Finland

²⁾ Department of Geosciences, University of Oslo, P.O. Box 1047 Blindern, N-0316 Oslo, Norway

Abstract

The southern Finnish Lapland area in the central part of the Fennoscandian shield is a geologically complex zone comprising several Archean blocks and Paleoproterozoic supracrustal belts all of which are intruded by voluminous Paleoproterozoic granites (the central Lapland granitoid complex, CLGC). New in-situ single crystal zircon U-Pb age determinations coupled with Lu-Hf isotope data from the same zircons were acquired from five granitoid rocks and one amphibolitic rock sample from the southern Lapland area. The samples represent at least four distinct magmatic events (at ca. 2.77 Ga, 2.12 Ga, 1.81 Ga, and 1.76 Ga). The 2.77 Ga and the 1.81-1.76 Ga events have initial Hf isotope signatures implying that local Archean rocks represent the source for the younger granites. The 2.12 Ga event has a slightly more juvenile Hf isotope composition suggesting either that the source for the 2.12 Ga granites represents a different Archean block or that the source is composed of mixed Archean and Paleoproterozoic components. The Neoarchean source for the Paleoproterozoic granites may be traced through the CLGC all the way to the Jokkmokk area in Sweden and possibly to the Lofoten area in Norway.

Keywords: granites, absolute age, zircon, Lu/Hf, U/Pb, magmatism, Archean, Proterozoic, Lapland, Finland

* Corresponding author email: laura.lauri@gtk.fi

Editorial handling: Arto Luttinen

1. Introduction

The isotopic composition of elements such as lead, strontium, neodymium, and hafnium in granites derived by partial melting of crustal rocks reflects the composition and history of their source.

Radiogenic isotope data from granitic rocks and their constituent minerals are therefore very useful indicators of the deep crustal sources of anatetic magma. Hf is a minor element in zircon, which is

an abundant, robust and datable accessory mineral in most granite intrusions. This makes the Lu–Hf isotope system in zircon an important indicator for granite petrogenesis and crustal evolution (e.g. Hawkesworth & Kemp, 2006; Andersen et al., 2009; Lauri et al., 2011).

Southern Finnish Lapland is a geologically complex area, where several Archean complexes and Paleoproterozoic supracrustal belts converge. The area has been overprinted by voluminous granite magmatism that obscures the pre-existing rocks and structures. In this study, we present new age determinations and Hf isotope data on six samples that cover a billion years of geological history of southern Finnish Lapland. Five of the samples represent different granitoid types of the study area and one sample is an amphibolite. In situ Hf isotope geochemistry combined with U–Pb age determinations from single crystal zircons allows us to see through the granite-forming event to determine the geological evolution of the area.

2. Geologic setting, sampling and petrography

The margin of the exposed Archean Karelian craton of the Fennoscandian shield lies in southern Lapland (Fig. 1 inset). The early Paleoproterozoic supracrustal belts of Peräpohja in the west and Kuusamo in the east overlay the old basement, which probably continues as a hidden crustal layer throughout northern Finland and into northern Sweden and Norway (see e.g., Mellqvist et al., 1999; Patison et al., 2006; Wade, 1995). The area on the northern side of the supracrustal belts hosts the Paleoproterozoic central Lapland granite complex (CLGC), which is geologically poorly known. Between the Peräpohja and Kuusamo belts the CLGC extends south towards the Archean Pudasjärvi complex (Fig. 1). The Suomujärvi complex (Fig. 1) is an Archean window or dome within the granite complex. It has been interpreted to be a part of the Belomorian province of the Fennoscandian shield (Evins et al., 2002). In the north, the CLGC is delimited by the Paleoproterozoic central Lapland greenstone belt.

Six samples were collected from the study area

(Fig. 1) for U–Pb age and Lu–Hf isotope analysis. The samples were chosen to represent igneous rocks with varying ages based on field mapping and available published data (e.g., Evins et al., 2002; Ahtonen et al., 2007).

Two samples were taken from the Suomujärvi Complex. The sample 109.1/JER/09 is a fine to

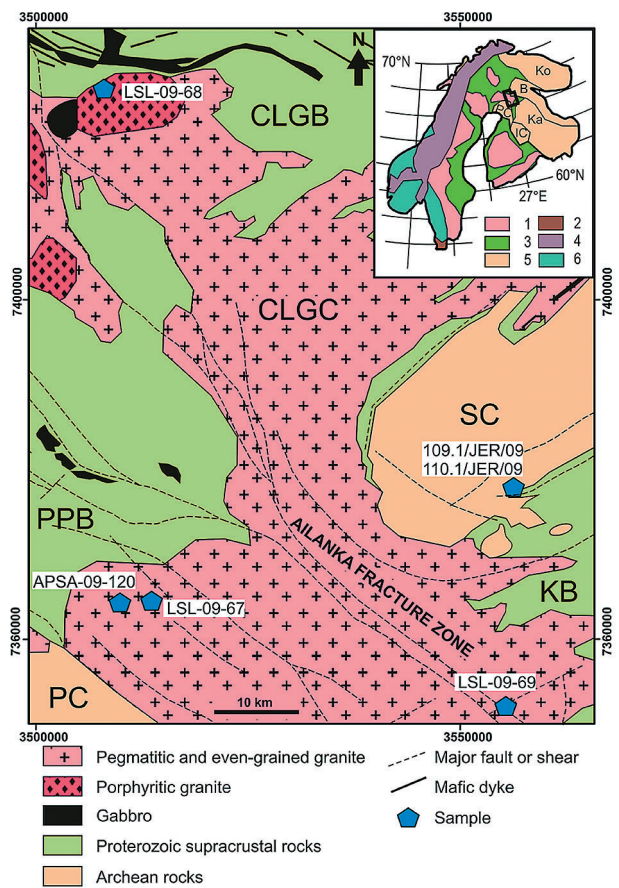


Fig. 1. Simplified geological map of the study area and the sampling locations (edited from the Digital Bedrock Map Database DigiKP, GTK). CLGC = Central Lapland Granite Complex, CLGB = Central Lapland greenstone belt, KB = Kuusamo belt, PC = Pudasjärvi complex, PPB = Peräpohja belt, SC = Suomujärvi complex. Coordinates according to the Finnish national grid (KKJ). Inset shows the simplified geological map of the Fennoscandian Shield. 1 = Paleoproterozoic igneous rocks, 2 = Phanerozoic rocks, 3 = Paleoproterozoic supracrustal rocks, 4 = Caledonian orogenic front, 5 = Archean rocks, 6 = Sveconorwegian rocks. Archean complexes: Ko = Kola, B = Belomoria, Ka = Karelia. IC = Iisalmi complex. PC = Pudasjärvi complex. Study area marked with a box.

medium-grained, dark gray amphibolite with a weak foliation (Fig. 2a). The major minerals are hornblende and plagioclase. Accessory minerals include magnetite, hematite, rutile, titanite, and zircon. The amphibolite also contains mm-scale silicic veinlets that consist of K-feldspar and quartz. The veinlets are oriented parallel to the schistosity. The amphibolite occurs as a dike or an inclusion within tonalitic to granodioritic gneiss (sample 110.1/JER/09), which is light gray, coarse-grained and shows a distinct gneissic fabric (Fig. 2b). Major minerals in the tonalite are plagioclase + quartz + biotite ± K-feldspar (microcline). Accessory magnetite occurs as visible crystals a few mm in diameter. Zircon and pyrite also occur as accessory minerals in the tonalite. The foliation in the rock is

defined by biotite. Quartz occurs as polycrystalline aggregates 3-6 mm in diameter. The gneiss fabric in the tonalite is cross-cut by silicic veins, which vary in thickness from mm to cm scale.

Four samples were taken from the granites that belong to the CLGC. The sample APSA-09-120 is fine-grained, gray, homogeneous granite that is surrounded by mica gneisses (Fig. 2c). No contact relations were observed due to lack of outcrop, but the granite was found in an area of several hundred square meters. Major minerals in the sample are K-feldspar + plagioclase + quartz + biotite. Rare larger K-feldspar crystals (up to 1 cm in diameter) are found in the otherwise equigranular granite. Accessory minerals include magnetite, zircon, uranothorite, uraninite, and allanite. Secondary sericite and

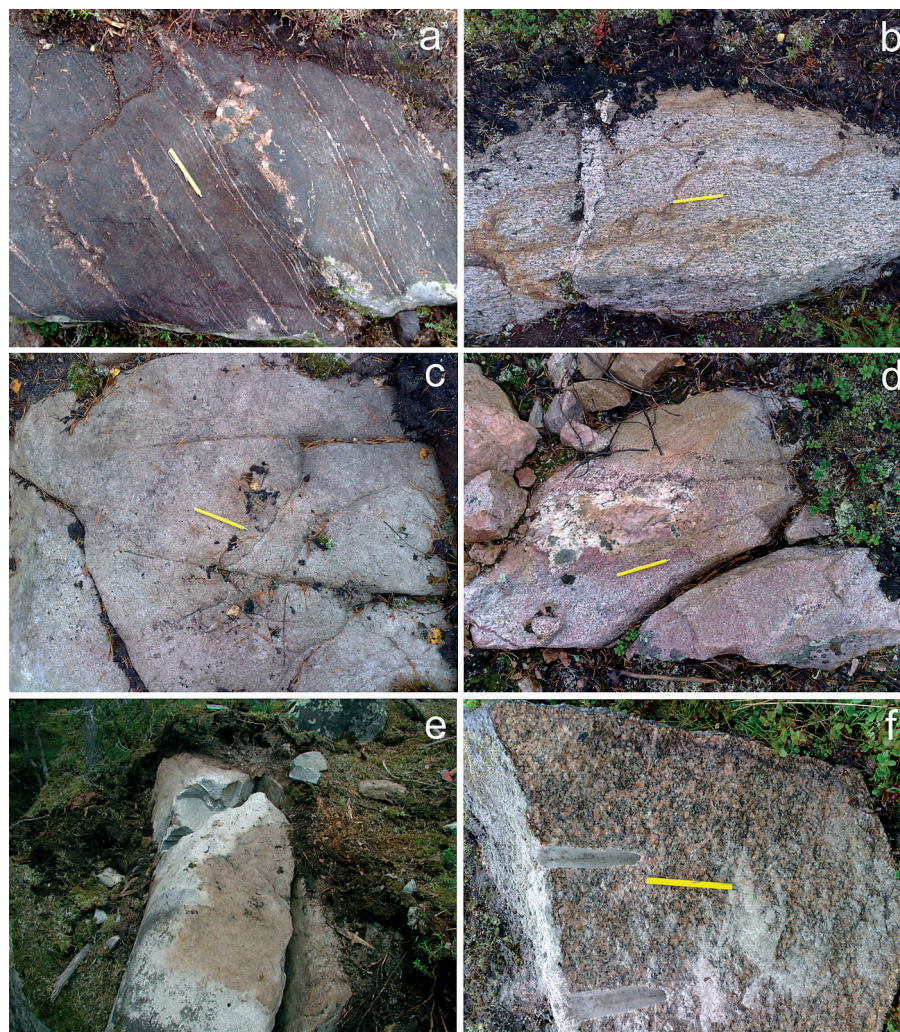


Fig. 2. Outcrop photos of (a) amphibolite 109.1/JER/09, (b) tonalite 110.1/JER/09, (c) granite APSA-09-120, (d) granite LSL-09-67, (e) granite LSL-09-69, (f) granite LSL-09-68. Yellow pen in photos a-d and f is ca. 12 cm long. Photo e is taken by J. Räsänen, all other photos taken by L.S. Lauri.

epidote are also common and biotite is somewhat chloritized. The sample LSL-09-69 is undeformed, fine-grained, gray granite (Fig. 2e) that resembles sample APSA-09-120. Major minerals are K-feldspar, quartz, plagioclase, and biotite. Accessory minerals include magnetite, allanite, zircon, and apatite. Secondary, fine-grained sericite and epidote are found along the grain boundaries and inside plagioclase crystals. The sample LSL-09-67 is a heterogeneous, pink leucogranite, in which the grain size varies from medium-grained to pegmatitic (Fig. 2d). The coarse-grained and pegmatitic types seem to intrude the medium-grained parts. A dated sample was taken from medium-grained granite. The major minerals in the medium-grained granite are K-feldspar, quartz, and plagioclase. Accessory minerals include biotite, rutile (as inclusions in biotite), uranothorite, zircon, and opaque minerals. Sericite, chlorite, and clinozoisite occur as secondary minerals. The sample LSL-09-68 is coarse-grained, porphyritic, red granite (Fig. 2f). Major minerals are K-feldspar (phenocrysts 1–2 cm in diameter) + quartz + plagioclase + biotite. Accessory minerals are magnetite, titanite, zircon, and allanite. Epidote occurs as a secondary phase. An unpublished TIMS U–Pb zircon age of ca. 1.79 Ga has been obtained from a porphyritic granite pluton in the vicinity (J. Räsänen, *unpublished data*).

2.1. Zircon

Zircon in the amphibolite sample 109.1/JER/09 forms short-prismatic, euhedral crystals which are bright and homogeneous in backscattered (BSE) electron images. The crystals do not show internal oscillatory zoning; BSE-dark rims and zones along

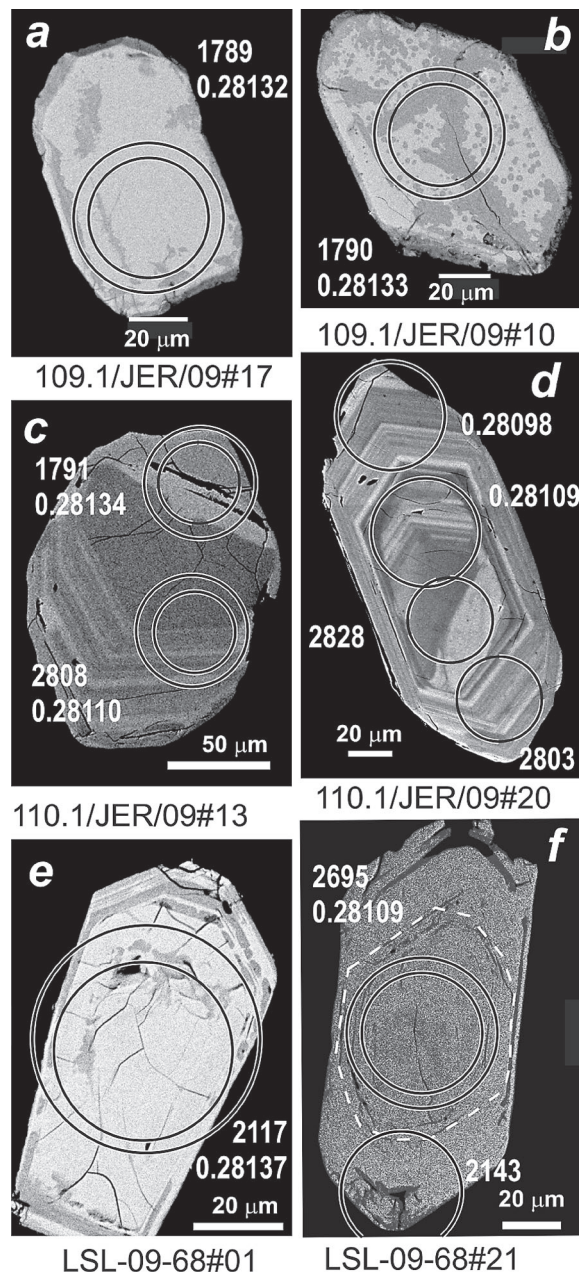


Fig. 3. Electron backscatter images of zircon. Circles represent the positions of U–Pb (small) and Lu–Hf (large) ablation spots. U–Pb was analysed first with low laser energy, leaving an ablation pit that was only ca. 10 µm deep. The digits after “#” refer to the number of analyses listed in Table 1. Numbers refer to ages in Ma and present-day $^{176}\text{Hf}/^{177}\text{Hf}$. (a) Internally homogeneous zircon crystal from the sample 109.1/JER/09. Note BSE dark zone along the rim, and minor, irregular patches of altered zircon. (b) Fractured and altered zircon from the sample 110.1/JER/09. An oscillatory zoned, Archean core has an irregular, BSE bright Proterozoic overgrowth. (c) Oscillatory zoned zircon with an apparent core, and a thin and discontinuous BSE-bright overgrowth, the sample 110.1/JER/09. There is no significant age difference from the apparent core to the main, oscillatory zoned part. (d) Euhedral zircon from the sample LSL-09-68. The central part of the crystal is homogeneous, whereas the rim shows oscillatory, magmatic zoning. (e) Euhedral zircon (sample LSL-09-68) with a core showing slightly BSE-darker patches (outline marked by a dashed line). The core has a Neoarchean age, whereas the rim is Paleoproterozoic.

fractures represent altered portions of the crystals (Fig. 3a, b). In the granitoid samples, crystal shapes vary from short-prismatic to elongated, with variably well-developed internal oscillatory zoning (Figs. 3c–e). Some crystals show oscillatory zoned cores overgrown by BSE-bright rims and embayments (Fig. 3c, d). Distinctly xenocrystic cores are rare (Fig. 3f).

3. Analytical methods

U–Pb and Lu–Hf analyses were made on single zircon crystals. Zircons were separated from crushed whole rock samples at the Department of Geosciences, University of Oslo by Wilfley table or gold pan washing and Frantz magnetic separation. Zircon grains selected by hand-picking were cast in epoxy mounts and polished. The zircons were imaged by backscattered electrons and cathodoluminescence in a scanning electron microscope prior to analysis. U–Pb and Lu–Hf isotope compositions were analyzed by laser-ablation inductively coupled plasma source mass spectrometry (LA-ICPMS) using a Nu Plasma HR mass spectrometer and a NewWave LUV213 laser microprobe at the Department of Geosciences, University of Oslo. The analytical protocol described in detail by Rosa et al. (2009) was used for U–Pb geochronology of zircon. A second-degree polynomial based on the three standards GJ-1 (609±1 Ma; Jackson et al., 2004), 91500 (1065±1 Ma; Wiedenbeck et al., 1995) and A382 (1877±2 Ma; H. Huhma, *pers. comm.*) was used to transform observed signal ratios to isotope ratios. U–Pb regressions were calculated using Isoplot Ex 3.59 (Ludwig, 2003). The long-term (> 2 years) precision is <1 % for $^{206}\text{Pb}/^{238}\text{U}$ and $^{207}\text{Pb}/^{206}\text{Pb}$ (2 standard deviations, SD).

Protocols for Lu–Hf isotope analysis follow Heinonen et al. (2010). The long-term value obtained for the Temora-2 reference zircon at 0.282679 ± 61 (2 SD, n = 460) indicates an analytical uncertainty of ± 2 epsilon units (TIMS-data: 0.282686 ± 0.000008; Woodhead & Hergt, 2005). The decay constant of ^{176}Lu of Söderlund et al. (2004), CHUR parameters of Bouvier et al. (2008) and Depleted Mantle parameters of Griffin et al. (2000), modified to the CHUR and λ values were used.

4. U–Pb geochronology

Sample 109.1/JER/09. Of the ten single zircons analyzed, eight were concordant within error at a concordia age of 1793±19 Ma (Fig. 4a, data from Table 1). The two remaining analyses are discordant, but with $^{207}\text{Pb}/^{206}\text{Pb}$ ages indistinguishable from the concordia age. The absence of oscillatory “magmatic” (e.g. Corfu et al., 2003) zoning in these zircons suggests that the 1793 Ma age reflects a metamorphic event, and thus the crystallization age of the protolith of the amphibolite remains uncertain.

Sample 110.1/JER/09. Zircon from this sample shows a significant variation in U–Pb characteristics, with groups of concordant or near-concordant analyses ranging from Archean to late Paleoproterozoic in age (Fig. 4b). A group of eight single grains are concordant at a concordia age of 2771±18 Ma, which is interpreted as the crystallization age of the tonalite. 14 discordant zircons give a weighted average $^{207}\text{Pb}/^{206}\text{Pb}$ age of 2796±16 Ma, indistinguishable from the concordia age. Two analyses of BSE-bright overgrowths (Fig. 3c) are slightly reversely discordant at 1750–1800 Ma, suggesting an event of secondary zircon growth in the sample at an age comparable to the presumably metamorphic age of 109.1/JER/09. The remaining four analyses scatter along a discordia line from this lower intercept to the Archean cluster.

Sample APSA-09-120. In APSA-09-120, nine of 25 analyzed zircons are concordant at a concordia age of 1761±8 Ma, which is interpreted as the crystallization age for the granite (Fig. 4c). The remaining zircons spread along a poorly defined lead-loss line to an imprecise, Phanerozoic lower intercept.

Sample LSL-09-69. Most zircons analyzed from this sample plot along a well-defined lead-loss line from an upper intercept at 1773±14 Ma to a Phanerozoic lower intercept (Fig. 4f); three of the zircons used to define the line are concordant at a concordia age of 1761±16 Ma, which is considered as the crystallization age for the granite. Two zircons plot to the right of the lead-loss line, suggesting inheritance from a Paleoproterozoic to late Archean source.

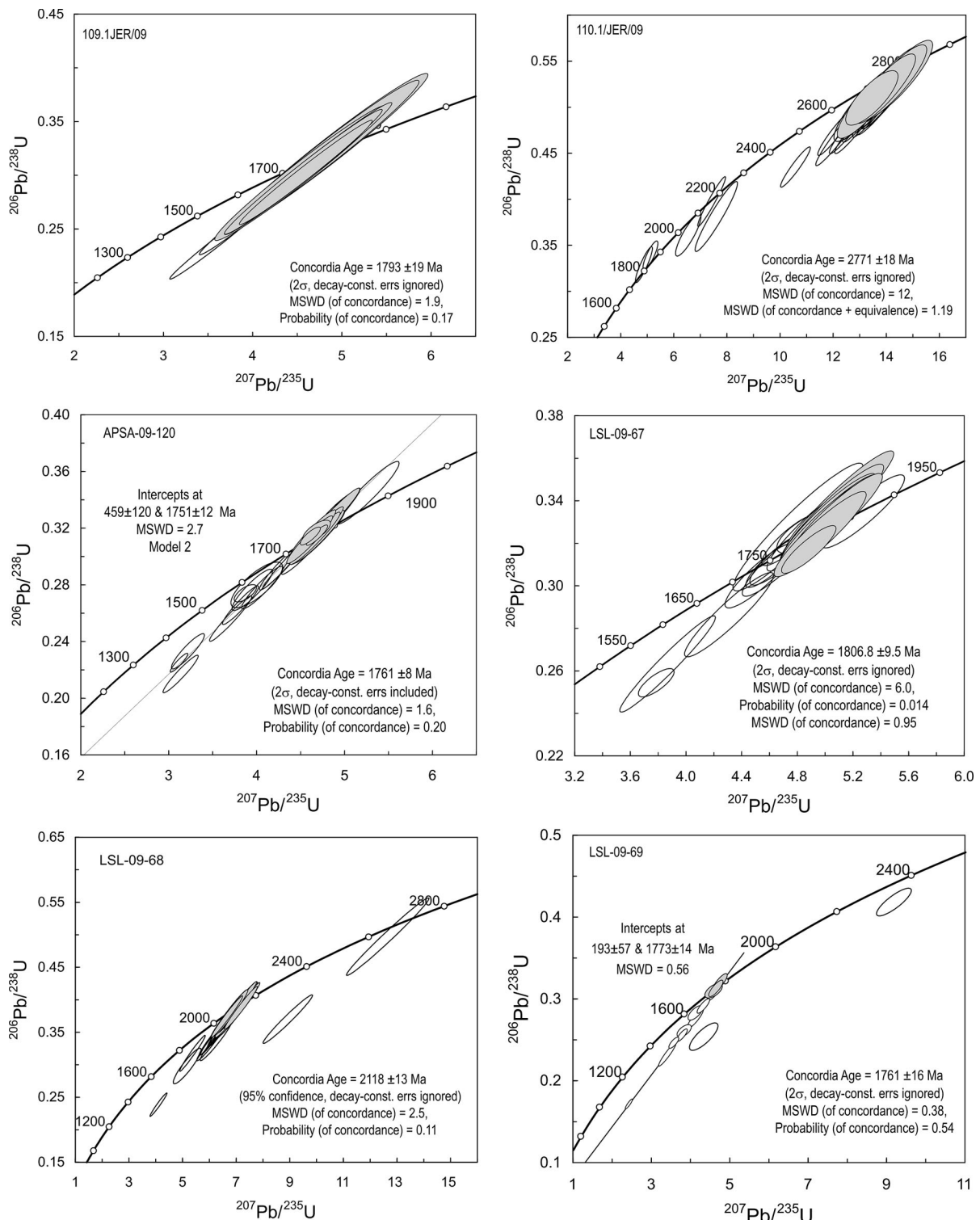


Fig. 4. U-Pb concordia diagrams, based on data from Table 1. Error ellipses are shown at 2 σ . Analyses shown in colour are used to calculate concordia ages for multi-grain populations. All calculations have been done using IsoplotEx 3.59 (Ludwig, 2003). See further explanation of the U-Pb relationships of the individual samples in the text.

Table 1 LAM-ICPMS U-Pb analyses of zircon from southern Lapland granite and amphibolite

| Sample | ppm | Ratios | | | | | | Discordance | Ages | | | | | | | | | | |
|---------------------|-----|--------|-------------------|----------------------------|--------------------------|----------------------------|----------|------------------------------------|---------|------------------------------------|-------|-------|----------------|--------------------|--------------------|--------------------|--------------------|--------------------|-----|
| | | U | ^{208}Pb | $^{203}\text{Pb}_c$ (%) | $^{206}/^{204}\text{Pb}$ | $^{206}/^{208}\text{Pb}^*$ | 1SE | $^{207}\text{Pb}/^{235}\text{U}^*$ | 1SE | $^{208}\text{Pb}/^{238}\text{U}^*$ | 1SE | Rho | Central (%) | Minimum rim (%) | 207/235 1 σ | 206/238 1 σ | 207/235 1 σ | 206/238 1 σ | |
| 109.1/JER/09 | | | | | | | | | | | | | | | | | | | |
| JER109_09 | 35 | 9.1 | 0.0 | 5016 | 0.10975 | 0.00097 | 3.62096 | 0.22497 | 0.23929 | 0.01472 | 0.990 | -25.5 | -23.1 | 1795 | 15 | 1554 | 49 | 1383 | 77 |
| JER109_10 | 33 | 9.7 | 0.0 | 13224 | 0.10943 | 0.00108 | 4.04992 | 0.26447 | 0.26847 | 0.01733 | 0.989 | -16.1 | -13.1 | 1790 | 17 | 1644 | 53 | 1533 | 88 |
| JER109_11 | 44 | 14.2 | 0.0 | 16257 | 0.11037 | 0.00112 | 4.59777 | 0.30551 | 0.30212 | 0.01984 | 0.988 | -6.5 | -3 | 1806 | 18 | 1749 | 55 | 1702 | 98 |
| JER109_12 | 45 | 14.2 | 0.0 | 10019 | 0.10954 | 0.00133 | 4.5709 | 0.36278 | 0.30664 | 0.02374 | 0.988 | -5.5 | -1.2 | 1792 | 21 | 1744 | 66 | 1704 | 117 |
| JER109_13 | 44 | 14.1 | 0.0 | 18129 | 0.10974 | 0.00141 | 4.62443 | 0.38418 | 0.30561 | 0.02508 | 0.988 | -4.8 | -0.2 | 1795 | 23 | 1754 | 69 | 1719 | 124 |
| JER109_16 | 56 | 17.9 | 0.0 | 15972 | 0.10922 | 0.00181 | 4.54257 | 0.39456 | 0.30164 | 0.02572 | 0.982 | -5.5 | . | 1786 | 29 | 1739 | 72 | 1699 | 127 |
| JER109_17 | 52 | 17.2 | 0.0 | 84808 | 0.10938 | 0.00189 | 4.811238 | 0.43245 | 0.3191 | 0.02814 | 0.981 | -0.2 | . | 1789 | 31 | 1787 | 76 | 1785 | 138 |
| JER109_19 | 56 | 18.8 | 0.0 | 18131 | 0.10954 | 0.00196 | 4.86492 | 0.4527 | 0.32211 | 0.02941 | 0.981 | 0.5 | . | 1792 | 31 | 1796 | 78 | 1800 | 143 |
| 110.1/JER/09 | | | | | | | | | | | | | | | | | | | |
| JER110_01_09c | 25 | 102.3 | 0.0 | 44033 | 0.19637 | 0.00334 | 14.22675 | 0.53184 | 0.52544 | 0.01741 | 0.886 | -3.2 | . | 2796 | 29 | 2765 | 35 | 2722 | 74 |
| JER110_01_11c | 17 | 65.8 | 0.0 | 13232 | 0.1907 | 0.00323 | 13.20341 | 0.47831 | 0.50216 | 0.01667 | 0.884 | -5.5 | -0.8 | 2748 | 28 | 2694 | 34 | 2623 | 69 |
| JER110_01_12c | 18 | 71.2 | 0.0 | 10586 | 0.19668 | 0.00349 | 14.25891 | 0.52164 | 0.52382 | 0.01683 | 0.875 | -3.3 | . | 2799 | 27 | 2767 | 35 | 2724 | 71 |
| JER110_01_13c | 19 | 78 | 0.0 | 11386 | 0.19783 | 0.00352 | 14.45903 | 0.53226 | 0.53008 | 0.01709 | 0.875 | -2.9 | . | 2808 | 28 | 2780 | 35 | 2742 | 72 |
| JER110_01_13r | 25 | 71.5 | 0.0 | 8678 | 0.10951 | 0.00135 | 5.12063 | 0.11467 | 0.33912 | 0.00635 | 0.836 | 5.9 | 0.9 | 1791 | 21 | 1840 | 19 | 1882 | 31 |
| JER110_01_16r | 28 | 115.6 | 0.2 | 5917 | 0.19161 | 0.00351 | 13.46007 | 0.40469 | 0.50948 | 0.01214 | 0.793 | -4.5 | . | 2756 | 29 | 2712 | 28 | 2654 | 52 |
| JER110_01_17c | 16 | 66.2 | 0.0 | 14476 | 0.19224 | 0.00353 | 13.47387 | 0.40347 | 0.50832 | 0.01203 | 0.79 | -4.9 | -0.2 | 2761 | 29 | 2713 | 28 | 2649 | 51 |
| JER110_01_23 | 23 | 94.7 | 0.0 | 15459 | 0.19476 | 0.00328 | 13.94967 | 0.47608 | 0.51946 | 0.01542 | 0.870 | -3.8 | . | 2783 | 28 | 2746 | 32 | 2697 | 65 |
| JER110_01_60 | 60 | 161.8 | 0.2 | 9231 | 0.13143 | 0.00197 | 6.54426 | 0.19507 | 0.36113 | 0.00931 | 0.865 | -7.1 | -2.4 | 2117 | 25 | 2052 | 26 | 1988 | 44 |
| JER110_01_12c | 12 | 50.4 | 0.0 | 11430 | 0.19643 | 0.00346 | 14.24594 | 0.503089 | 0.526 | 0.01727 | 0.881 | -3.2 | . | 2797 | 29 | 2766 | 35 | 2725 | 73 |
| JER110_01_03c | 29 | 117 | 0.0 | 27990 | 0.19524 | 0.00342 | 14.10544 | 0.52339 | 0.52397 | 0.01723 | 0.883 | -3.1 | . | 2787 | 29 | 2757 | 35 | 2716 | 73 |
| JER110_01_06c | 13 | 50.6 | 0.0 | 7100 | 0.19153 | 0.00331 | 13.33933 | 0.48283 | 0.50511 | 0.01667 | 0.879 | -5.3 | -0.4 | 2755 | 27 | 2704 | 34 | 2636 | 69 |
| JER110_01_08c | 110 | 270.3 | 0.0 | 18605 | 0.14457 | 0.00197 | 7.60003 | 0.32592 | 0.38129 | 0.0155 | 0.948 | -10.3 | -6.1 | 2283 | 22 | 2185 | 38 | 2082 | 72 |
| JER110_01_08r | 84 | 207 | 0.0 | 45424 | 0.10744 | 0.00124 | 4.87376 | 0.13071 | 0.32299 | 0.00796 | 0.902 | 5 | . | 1757 | 20 | 1798 | 23 | 1833 | 39 |
| JER110_01_18c | 35 | 48.8 | 0.1 | 9782 | 0.18901 | 0.00156 | 1.237603 | 0.42143 | 0.47449 | 0.01569 | 0.970 | -10.1 | -7.8 | 2734 | 14 | 2633 | 32 | 2505 | 69 |
| JER110_01_19c | 61 | 84.5 | 0.0 | 37393 | 0.1933 | 0.00143 | 13.18235 | 0.39398 | 0.49461 | 0.01222 | 0.958 | -7.9 | -5.8 | 2770 | 12 | 2693 | 24 | 2591 | 53 |
| JER110_01_20c | 41 | 58.7 | 0.0 | 18303 | 0.20024 | 0.00153 | 14.05156 | 0.37318 | 0.50893 | 0.01295 | 0.958 | -7.6 | -5.5 | 2828 | 12 | 2753 | 25 | 2652 | 55 |
| JER110_01_20r | 52 | 73.4 | 0.0 | 33009 | 0.19714 | 0.00149 | 13.69968 | 0.36085 | 0.50401 | 0.01272 | 0.958 | -7.5 | -5.3 | 2803 | 12 | 2729 | 25 | 2631 | 55 |
| JER110_01_21c | 34 | 45.9 | 0.0 | 26919 | 0.19185 | 0.00142 | 12.64133 | 0.311974 | 0.47788 | 0.011155 | 0.956 | -10.5 | -8.5 | 2758 | 12 | 2653 | 24 | 2518 | 50 |
| JER110_01_23c | 45 | 57.8 | 0.0 | 15208 | 0.18562 | 0.00133 | 12.08494 | 0.27113 | 0.47219 | 0.0104 | 0.947 | -9.4 | -7.4 | 2704 | 11 | 2611 | 21 | 2493 | 44 |
| JER110_01_23r | 133 | 128.4 | 0.3 | 4303 | 0.13543 | 0.00103 | 7.42449 | 0.21337 | 0.3976 | 0.01103 | 0.964 | -0.6 | . | 2170 | 13 | 2164 | 26 | 2158 | 51 |
| JER110_01_24c | 39 | 53.8 | 0.0 | 90664 | 0.19798 | 0.00144 | 13.49754 | 0.31508 | 0.49447 | 0.01097 | 0.951 | -9.5 | -7.5 | 2810 | 11 | 2715 | 22 | 2590 | 47 |
| JER110_01_24r | 55 | 77.9 | 0.0 | 25190 | 0.1981 | 0.00143 | 14.00962 | 0.33697 | 0.5129 | 0.01177 | 0.954 | -6.2 | -4.1 | 2811 | 11 | 2750 | 23 | 2669 | 50 |
| JER110_01_28c | 44 | 61 | 0.0 | 21902 | 0.19841 | 0.00144 | 13.83022 | 0.32898 | 0.50555 | 0.01145 | 0.952 | -7.6 | -5.6 | 2813 | 12 | 2738 | 23 | 2638 | 49 |
| JER110_01_61c | 36 | 47.8 | 0.0 | 11163 | 0.19974 | 0.00155 | 13.81035 | 0.36916 | 0.50147 | 0.01283 | 0.957 | -8.8 | -6.7 | 2824 | 12 | 2737 | 25 | 2620 | 55 |
| JER110_01_62c | 57 | 66.8 | 0.0 | 16597 | 0.1764 | 0.00121 | 10.58025 | 0.22958 | 0.435 | 0.00875 | 0.949 | -13.2 | -11.4 | 2619 | 11 | 2487 | 20 | 2328 | 40 |
| JER110_01_63c | 45 | 63.6 | 0.5 | 2412 | 0.19974 | 0.00148 | 13.90823 | 0.33839 | 0.50301 | 0.01171 | 0.953 | -8.1 | -6.1 | 2824 | 12 | 2743 | 23 | 2635 | 50 |
| JER110_01_64c | 43 | 55.4 | 0.0 | 15292 | 0.19515 | 0.00142 | 12.78856 | 0.29962 | 0.47578 | 0.01047 | 0.95 | -12.1 | -10.1 | 2786 | 11 | 2664 | 22 | 2507 | 46 |
| JER110_01_65 | 30 | 39.9 | 0.0 | 10209 | 0.19458 | 0.00145 | 13.11395 | 0.30984 | 0.48882 | 0.01096 | 0.949 | -9.4 | -7.3 | 2781 | 12 | 2688 | 22 | 2566 | 47 |

▶

| Sample | ppm | | | Ratios | | | Discordance | | | Ages | | | | | | | | |
|---------------|-----|-------------------|----------------------------|---------|---------|-------------------------------------|-------------|------------------------------------|---------|------------------------------------|-------|-------|----------------|--------------------|--------------------|--------------------|------|------|
| | U | ^{206}Pb | $^{206}\text{Pb}_c$ (%) | 206/204 | 206/204 | $^{207}\text{Pb}/^{206}\text{Pb}^*$ | 1SE | $^{207}\text{Pb}/^{235}\text{U}^*$ | 1SE | $^{206}\text{Pb}/^{238}\text{U}^*$ | 1SE | Rho | Central (%) | Minimum rim (%) | 207/235 1 σ | 206/238 1 σ | | |
| Analysis no | | | | | | | | | | | | | | | | | | |
| APSA-09-120 | | | | | | | | | | | | | | | | | | |
| APSA-01 | 98 | 141.6 | 2.5 | 620 | 0.10683 | 0.00105 | 4.68556 | 0.06487 | 0.31811 | 0.00309 | 0.702 | 2.3 | . | 1746 | 17 | 1765 | 12 | 1781 |
| APSA-02 | 130 | 183.1 | 0.0 | 64741 | 0.10801 | 0.00052 | 4.69046 | 0.04927 | 0.31495 | 0.00294 | 0.889 | -0.1 | . | 1766 | 8 | 1766 | 9 | 1765 |
| APSA-03 | 491 | 698.1 | 0.0 | 128262 | 0.10647 | 0.00058 | 4.61633 | 0.04593 | 0.31447 | 0.00262 | 0.837 | 1.5 | . | 1740 | 10 | 1752 | 8 | 1763 |
| APSA-04 | 276 | 419.3 | 0.0 | 129434 | 0.10667 | 0.00056 | 4.78236 | 0.05452 | 0.32515 | 0.00329 | 0.889 | 4.7 | 2.2 | 1743 | 9 | 1782 | 10 | 1815 |
| APSA-05 | 176 | 264 | 0.0 | 75634 | 0.10705 | 0.00052 | 4.95953 | 0.05087 | 0.336 | 0.00304 | 0.883 | 7.7 | 5.4 | 1750 | 9 | 1812 | 9 | 1867 |
| APSA-08 | 337 | 324.5 | 0.3 | 5425 | 0.10044 | 0.0005 | 3.11706 | 0.04084 | 0.22507 | 0.00273 | 0.924 | -21.9 | -20.3 | 1632 | 9 | 1437 | 10 | 1309 |
| APSA-09 | 90 | 109.6 | 3.4 | 452 | 0.10245 | 0.00101 | 3.87132 | 0.05194 | 0.27407 | 0.0025 | 0.680 | -7.2 | -4.3 | 1669 | 17 | 1608 | 11 | 1561 |
| APSA-10 | 170 | 119.9 | 0.8 | 1964 | 0.10601 | 0.00089 | 4.06562 | 0.09632 | 0.27815 | 0.00616 | 0.935 | -9.8 | -6.7 | 1732 | 15 | 1647 | 19 | 1582 |
| APSA-11 | 513 | 422.9 | 0.0 | 61099 | 0.10742 | 0.00084 | 4.87604 | 0.10821 | 0.3292 | 0.00684 | 0.936 | 5.1 | 0.1 | 1756 | 13 | 1798 | 19 | 1835 |
| APSA-12 | 201 | 138.8 | 0.0 | 42103 | 0.10608 | 0.00073 | 4.28732 | 0.10433 | 0.29312 | 0.00684 | 0.959 | -5 | -2.4 | 1733 | 12 | 1691 | 20 | 1657 |
| APSA-13 | 287 | 236.3 | 0.0 | 46694 | 0.10661 | 0.00075 | 4.64497 | 0.1071 | 0.316 | 0.00654 | 0.953 | 1.8 | . | 1742 | 13 | 1757 | 19 | 1770 |
| APSA-14 | 226 | 166.1 | 1.4 | 1174 | 0.10363 | 0.00107 | 3.95049 | 0.09438 | 0.27649 | 0.00595 | 0.901 | -7.8 | -4 | 1690 | 19 | 1624 | 19 | 1574 |
| APSA-15 | 359 | 290.3 | 0.0 | 57311 | 0.10719 | 0.00077 | 4.60832 | 0.10635 | 0.3118 | 0.00684 | 0.951 | -0.2 | . | 1752 | 13 | 1751 | 19 | 1750 |
| APSA-17 | 204 | 203.6 | 0.0 | 52672 | 0.11065 | 0.00103 | 5.26326 | 0.14617 | 0.34478 | 0.00903 | 0.942 | 6.4 | 1.1 | 1810 | 17 | 1833 | 24 | 1911 |
| APSA-18 | 145 | 99.6 | 4.4 | 344 | 0.10011 | 0.00097 | 3.21831 | 0.07681 | 0.23315 | 0.00568 | 0.914 | -18.7 | -15.5 | 1626 | 18 | 1462 | 18 | 1351 |
| APSA-20_end | 266 | 175.8 | 0.0 | 8367 | 0.10473 | 0.00082 | 3.13583 | 0.08187 | 0.21716 | 0.00541 | 0.954 | -28.5 | -26.2 | 1710 | 14 | 1442 | 20 | 1267 |
| APSA-20_front | 348 | 230.7 | 0.1 | 13736 | 0.10651 | 0.00049 | 4.35517 | 0.11734 | 0.29556 | 0.00787 | 0.985 | -4.3 | -2.6 | 1741 | 8 | 1704 | 22 | 1674 |
| APSA-21 | 130 | 91.8 | 0.6 | 2311 | 0.10834 | 0.0008 | 4.57934 | 0.12183 | 0.30657 | 0.00784 | 0.961 | -3.1 | -0.3 | 1772 | 13 | 1746 | 22 | 1724 |
| APSA-22 | 361 | 290.1 | 0.2 | 5543 | 0.10873 | 0.00083 | 4.70797 | 0.12008 | 0.31403 | 0.00764 | 0.954 | -1.1 | . | 1778 | 14 | 1769 | 21 | 1761 |
| APSA-24 | 154 | 101.9 | 2.6 | 582 | 0.10421 | 0.00071 | 0.08409 | 0.26668 | 0.00357 | 0.951 | -12 | -9.6 | 1700 | 12 | 1596 | 18 | 1519 | |
| APSA-25 | 196 | 167.4 | 0.1 | 18022 | 0.10762 | 0.00072 | 4.87421 | 0.12408 | 0.32849 | 0.00807 | 0.965 | 4.7 | . | 1759 | 12 | 1798 | 21 | 1831 |
| APSA-26 | 177 | 144.4 | 0.0 | 80005 | 0.10785 | 0.00073 | 4.70555 | 0.11768 | 0.31657 | 0.00762 | 0.963 | 0.7 | . | 1763 | 12 | 1768 | 21 | 1773 |
| APSA-27 | 234 | 189.1 | 0.0 | 22008 | 0.10825 | 0.00074 | 4.67111 | 0.11713 | 0.31295 | 0.00755 | 0.962 | -1 | . | 1770 | 12 | 1762 | 21 | 1755 |
| APSA-28 | 91 | 68 | 4.3 | 407 | 0.10362 | 0.00193 | 4.00103 | 0.11918 | 0.28003 | 0.00657 | 0.783 | -6.6 | -0.3 | 1690 | 33 | 1634 | 24 | 1592 |
| APSA-29 | 330 | 217.6 | 0.8 | 1829 | 0.10487 | 0.00073 | 3.70463 | 0.09832 | 0.2562 | 0.00656 | 0.965 | -15.8 | -13.4 | 1712 | 12 | 1572 | 21 | 1470 |
| LSL-09-67 | | | | | | | | | | | | | | | | | | |
| LSL67-01 | 38 | 91.3 | 0.0 | 11201 | 0.11162 | 0.00088 | 4.88164 | 0.08038 | 0.31719 | 0.00458 | 0.878 | -3.1 | -0.3 | 1826 | 14 | 1799 | 14 | 1776 |
| LSL67-04 | 79 | 187.2 | 0.4 | 3892 | 0.10794 | 0.00087 | 4.62657 | 0.07997 | 0.31087 | 0.00475 | 0.884 | -1.3 | . | 1765 | 14 | 1754 | 14 | 1745 |
| LSL67-04b | 55 | 129.9 | 0.4 | 3950 | 0.10837 | 0.00101 | 4.67068 | 0.0866 | 0.31227 | 0.00501 | 0.864 | -1.2 | . | 1772 | 16 | 1762 | 16 | 1753 |
| LSL67-05 | 77 | 189.3 | 1.4 | 959 | 0.10711 | 0.00093 | 4.74736 | 0.08288 | 0.32146 | 0.00487 | 0.868 | 3 | . | 1751 | 15 | 1776 | 15 | 1797 |
| LSL67-06r | 110 | 207.8 | 0.4 | 2360 | 0.10793 | 0.00096 | 3.78759 | 0.05245 | 0.25441 | 0.00271 | 0.769 | -19.2 | -16.8 | 1685 | 15 | 1590 | 11 | 1461 |
| LSL67-07 | 43 | 107.1 | 0.0 | 1835 | 0.11145 | 0.00112 | 5.27259 | 0.12193 | 0.335 | 0.00701 | 0.905 | -0.2 | . | 1764 | 19 | 1737 | 19 | 1715 |
| LSL67-08 | 69 | 100.8 | 1.4 | 1030 | 0.10912 | 0.00119 | 4.30938 | 0.13052 | 0.28643 | 0.00809 | 0.933 | -10.2 | -6.4 | 1785 | 20 | 1695 | 25 | 1624 |
| LSL67-10c | 171 | 303.6 | 0.0 | 68491 | 0.10949 | 0.00112 | 5.06677 | 0.12352 | 0.33164 | 0.00738 | 0.909 | 3.6 | . | 1791 | 19 | 1820 | 21 | 1846 |
| LSL67-10r | 120 | 214.3 | 0.2 | 9475 | 0.10921 | 0.00115 | 4.9971 | 0.11465 | 0.33185 | 0.00677 | 0.889 | 3.9 | . | 1791 | 17 | 1823 | 22 | 1852 |
| LSL67-11 | 56 | 92.8 | 1.3 | 51009 | 0.11024 | 0.00111 | 4.53335 | 0.10324 | 0.30476 | 0.00619 | 0.891 | -3.2 | . | 1803 | 18 | 1823 | 25 | 1839 |
| LSL67-12 | 49 | 80.8 | 0.6 | 2315 | 0.10887 | 0.00108 | 4.67329 | 0.12193 | 0.31133 | 0.00643 | 0.906 | -2.1 | . | 1781 | 18 | 1762 | 20 | 1827 |
| LSL67-13 | 68 | 119 | 0.0 | 19190 | 0.10967 | 0.00111 | 4.0281 | 0.12289 | 0.30899 | 0.0078 | 0.921 | 2.8 | . | 1794 | 17 | 1818 | 22 | 1838 |
| LSL67-15 | 154 | 270.7 | 0.1 | 26521 | 0.10947 | 0.00109 | 5.02251 | 0.13056 | 0.33275 | 0.00799 | 0.924 | 3.9 | . | 1791 | 17 | 1823 | 22 | 1852 |
| LSL67-16 | 64 | 110.5 | 0.0 | 51009 | 0.11024 | 0.00111 | 5.01909 | 0.14225 | 0.3302 | 0.00924 | 0.939 | 2.3 | . | 1803 | 18 | 1823 | 25 | 1839 |
| LSL67-17 | 107 | 172.8 | 2.6 | 582 | 0.10637 | 0.00144 | 4.80534 | 0.19115 | 0.32264 | 0.01226 | 0.941 | 5.9 | . | 1738 | 24 | 1786 | 33 | 1827 |
| LSL67-18 | 80 | 149.2 | 1.0 | 1569 | 0.10837 | 0.00129 | 4.85623 | 0.08301 | 0.32501 | 0.00398 | 0.716 | 2.7 | . | 1772 | 22 | 1795 | 14 | 1814 |
| LSL67-20 | 305 | 388.1 | 0.0 | 25373 | 0.10658 | 0.00099 | 3.86832 | 0.14039 | 0.26324 | 0.00967 | -15.1 | -12 | . | 1742 | 16 | 1607 | 29 | 1506 |
| LSL67-21 | 144 | 252.3 | 0.0 | 47337 | 0.10913 | 0.00112 | 5.09864 | 0.16006 | 0.33887 | 0.0106 | 0.945 | 6.2 | . | 1785 | 18 | 1836 | 27 | 1881 |
| LSL67-22 | 241 | 424.8 | 0.0 | 18838 | 0.10947 | 0.00112 | 5.07859 | 0.13859 | 0.33647 | 0.00852 | 0.927 | 5.1 | . | 1791 | 17 | 1833 | 23 | 1870 |

| | | | | | | | | | | | | | | | | | | | |
|------------------|-----|-------|-----|-------|---------|---------|----------|---------|---------|---------|-------|-------|-------|------|----|------|----|------|-----|
| LSL67-23 | 152 | 264.9 | 0.0 | 9695 | 0.1107 | 0.00115 | 5.06832 | 0.13941 | 0.33205 | 0.00846 | 0.926 | 2.4 | . | 1811 | 18 | 1831 | 23 | 1848 | 41 |
| LSL67-24 | 191 | 332.8 | 0.0 | 16490 | 0.10973 | 0.00113 | 5.02429 | 0.13828 | 0.33208 | 0.00847 | 0.927 | 3.4 | . | 1795 | 18 | 1823 | 23 | 1848 | 41 |
| LSL67-25 | 136 | 235.2 | 0.0 | 26249 | 0.11025 | 0.00115 | 5.00868 | 0.13806 | 0.3295 | 0.00841 | 0.926 | 2.1 | . | 1804 | 18 | 1821 | 23 | 1836 | 41 |
| LSL67-26 | 176 | 304.4 | 0.4 | 3671 | 0.10884 | 0.00112 | 4.90986 | 0.13415 | 0.32716 | 0.00828 | 0.926 | 2.9 | . | 1780 | 18 | 1804 | 23 | 1825 | 40 |
| LSL67-27 | 112 | 189.7 | 0.0 | 11375 | 0.11092 | 0.00115 | 4.96129 | 0.13533 | 0.3244 | 0.00819 | 0.926 | -0.2 | . | 1815 | 18 | 1813 | 23 | 1811 | 40 |
| LSL-09-68 | | | | | | | | | | | | | | | | | | | |
| LSL0968-01 | 51 | 100.7 | 0.0 | 13007 | 0.13144 | 0.00116 | 6.05811 | 0.21526 | 0.32427 | 0.0115 | 0.969 | -14 | -11.4 | 2117 | 15 | 1984 | 31 | 1859 | 56 |
| LSL0968-02 | 50 | 119.6 | 0.0 | 59332 | 0.13135 | 0.00106 | 6.99058 | 0.28128 | 0.38558 | 0.01521 | 0.980 | -0.7 | . | 2116 | 13 | 2110 | 36 | 2104 | 71 |
| LSL0968-03 | 29 | 65.5 | 0.0 | 8550 | 0.13356 | 0.00121 | 6.96218 | 0.2731 | 0.37806 | 0.01443 | 0.973 | -4.3 | -1.3 | 2145 | 15 | 2107 | 35 | 2067 | 68 |
| LSL0968-05 | 49 | 112.8 | 0.0 | 41928 | 0.12945 | 0.00119 | 6.77502 | 0.26867 | 0.37959 | 0.01464 | 0.973 | -0.9 | . | 2090 | 16 | 2082 | 35 | 2074 | 68 |
| LSL0968-07 | 33 | 66.3 | 0.0 | 6544 | 0.13443 | 0.00136 | 6.25007 | 0.24194 | 0.33772 | 0.0126 | 0.965 | -15.1 | -12.1 | 2157 | 17 | 2011 | 34 | 1873 | 61 |
| LSL0968-08 | 43 | 98.5 | 0.0 | 28583 | 0.13205 | 0.00131 | 6.96709 | 0.28633 | 0.37937 | 0.01527 | 0.971 | -2.9 | . | 2125 | 17 | 2100 | 37 | 2073 | 71 |
| LSL0968-09 | 33 | 76.2 | 0.0 | 19193 | 0.13316 | 0.00126 | 6.99266 | 0.29406 | 0.38086 | 0.01463 | 0.974 | -3.3 | -0.1 | 2140 | 17 | 2110 | 37 | 2080 | 73 |
| LSL0968-10 | 49 | 108.1 | 0.1 | 16064 | 0.13194 | 0.00121 | 6.60524 | 0.27729 | 0.3631 | 0.01463 | 0.975 | -7 | -4 | 2124 | 16 | 2060 | 36 | 1997 | 69 |
| LSL0968-11 | 30 | 65.9 | 0.0 | 37998 | 0.13175 | 0.00117 | 6.65539 | 0.26593 | 0.36638 | 0.01427 | 0.975 | -6 | -3.1 | 2121 | 16 | 2067 | 35 | 2012 | 67 |
| LSL0968-12 | 27 | 47.9 | 3.0 | 1138 | 0.12587 | 0.00209 | 5.17317 | 0.21179 | 0.29808 | 0.01116 | 0.914 | -20 | -15.2 | 2041 | 28 | 1848 | 35 | 1682 | 55 |
| LSL0968-13 | 47 | 109.9 | 0.0 | 24127 | 0.13152 | 0.00115 | 7.00908 | 0.30978 | 0.38651 | 0.01674 | 0.98 | -0.7 | . | 2118 | 14 | 2113 | 39 | 2107 | 78 |
| LSL0968-14a | 241 | 147.9 | 0.1 | 15447 | 0.13209 | 0.00092 | 6.776779 | 0.24213 | 0.37209 | 0.01304 | 0.981 | -4.8 | -2.5 | 2126 | 12 | 2083 | 32 | 2039 | 61 |
| LSL0968-14b | 187 | 114.9 | 0.0 | 15631 | 0.12878 | 0.00088 | 6.635551 | 0.23733 | 0.37369 | 0.01312 | 0.981 | -1.9 | . | 2081 | 12 | 2064 | 32 | 2047 | 62 |
| LSL0968-15 | 68 | 38.3 | 0.3 | 8669 | 0.12991 | 0.00091 | 6.11885 | 0.20698 | 0.34161 | 0.01351 | 0.978 | -11.1 | -9 | 2097 | 12 | 1993 | 30 | 1894 | 54 |
| LSL0968-17 | 41 | 26 | 0.1 | 8890 | 0.13419 | 0.00097 | 7.16642 | 0.25537 | 0.38734 | 0.01351 | 0.979 | -2.3 | . | 2153 | 12 | 2132 | 32 | 2110 | 63 |
| LSL0968-20 | 105 | 62.6 | 0.2 | 8156 | 0.13147 | 0.00092 | 6.6592 | 0.25573 | 0.36736 | 0.01387 | 0.983 | -5.5 | -3.3 | 2118 | 12 | 2067 | 34 | 2017 | 65 |
| LSL0968-21c | 67 | 54.8 | 0.0 | 34240 | 0.18466 | 0.00148 | 1.265665 | 0.62926 | 0.49711 | 0.02441 | 0.987 | -4.2 | -2 | 2695 | 13 | 2654 | 47 | 2601 | 105 |
| LSL0968-21r | 130 | 82.1 | 0.0 | 8420 | 0.13341 | 0.00099 | 6.99712 | 0.23459 | 0.38038 | 0.01244 | 0.975 | -3.6 | -1.1 | 2143 | 12 | 2111 | 30 | 2078 | 58 |
| LSL0968-22 | 88 | 55.5 | 0.0 | 19245 | 0.13141 | 0.00089 | 7.07433 | 0.27735 | 0.39045 | 0.01519 | 0.985 | 0.4 | . | 2117 | 12 | 2121 | 35 | 2125 | 70 |
| LSL0968-27c | 106 | 40.5 | 1.8 | 812 | 0.12467 | 0.00084 | 4.10243 | 0.12982 | 0.23865 | 0.00738 | 0.977 | -35.3 | -33.8 | 2024 | 11 | 1655 | 26 | 1380 | 38 |
| LSL0968-31c | 64 | 32.7 | 2.3 | 626 | 0.12258 | 0.00087 | 5.36917 | 0.19484 | 0.31767 | 0.01131 | 0.981 | -12.4 | -10.2 | 1994 | 12 | 1880 | 31 | 1778 | 55 |
| LSL0968-37 | 115 | 64.5 | 0.0 | 32729 | 0.13071 | 0.00097 | 6.14845 | 0.19515 | 0.34115 | 0.01053 | 0.972 | -11.8 | -9.5 | 2108 | 13 | 1997 | 28 | 1892 | 51 |
| LSL0968-40 | 96 | 60.6 | 0.0 | 7885 | 0.13426 | 0.00097 | 7.1482 | 0.26107 | 0.38616 | 0.01382 | 0.98 | -2.7 | -0.3 | 2154 | 12 | 2130 | 33 | 2105 | 64 |
| LSL0968-79 | 30 | 17.6 | 0.1 | 9412 | 0.17489 | 0.00154 | 8.92775 | 0.37732 | 0.37022 | 0.01533 | 0.978 | -25.7 | -23.6 | 2605 | 14 | 2331 | 39 | 2030 | 72 |
| LSL0968-82 | 144 | 87.7 | 0.0 | 4931 | 0.13353 | 0.001 | 7.10683 | 0.30687 | 0.38601 | 0.01642 | 0.985 | -2.2 | . | 2145 | 13 | 2125 | 38 | 2104 | 76 |
| LSL-09-69 | | | | | | | | | | | | | | | | | | | |
| CLGC_0110_03 | 231 | 73.9 | 0.2 | 66071 | 0.10802 | 0.00098 | 4.75361 | 0.07786 | 0.31916 | 0.00435 | 0.833 | 1.2 | . | 1766 | 15 | 1777 | 14 | 1786 | 21 |
| CLGC_0110_04 | 86 | 26.9 | 0.0 | 17858 | 0.10803 | 0.00099 | 4.65267 | 0.07472 | 0.31236 | 0.00411 | 0.820 | -0.9 | . | 1766 | 16 | 1759 | 13 | 1752 | 20 |
| CLGC_0110_05 | 273 | 60.8 | 0.7 | 2281 | 0.10676 | 0.00092 | 3.40947 | 0.09063 | 0.23162 | 0.00582 | 0.946 | -25.5 | -22.9 | 1745 | 15 | 1507 | 21 | 1343 | 30 |
| CLGC_0110_06 | 291 | 89.2 | 0.2 | 8630 | 0.10881 | 0.00092 | 4.6121 | 0.073 | 0.30743 | 0.00412 | 0.847 | 0.847 | . | 1780 | 15 | 1751 | 13 | 1728 | 20 |
| CLGC_0110_07 | 535 | 135.7 | 0.4 | 6148 | 0.10764 | 0.00091 | 3.78721 | 0.05571 | 0.25518 | 0.00303 | 0.820 | -18.7 | -16.3 | 1760 | 15 | 1590 | 12 | 1465 | 16 |
| CLGC_0110_08 | 225 | 65.6 | 0.6 | 2166 | 0.10793 | 0.00091 | 4.3295 | 0.06649 | 0.29093 | 0.00374 | 0.837 | -7.6 | -4.8 | 1765 | 15 | 1699 | 13 | 1646 | 19 |
| CLGC_0110_09 | 242 | 103.3 | 0.7 | 2050 | 0.1593 | 0.00172 | 9.18919 | 0.18126 | 0.41836 | 0.00691 | 0.837 | -9.4 | -6.5 | 2448 | 18 | 2357 | 18 | 2253 | 31 |
| CLGC0110_01 | 135 | 36.9 | 0.2 | 6744 | 0.10858 | 0.00101 | 4.12695 | 0.08271 | 0.27556 | 0.00489 | 0.885 | -13.1 | -10 | 1776 | 16 | 1660 | 16 | 1569 | 25 |
| CLGC0110_02 | 726 | 177.8 | 0.3 | 4991 | 0.10551 | 0.00096 | 3.57935 | 0.05199 | 0.24603 | 0.00278 | 0.777 | -19.7 | -17.2 | 1723 | 16 | 1545 | 12 | 1418 | 14 |
| CLGC_0110_10 | 102 | 29.4 | 1.5 | 887 | 0.10611 | 0.00142 | 4.12627 | 0.07628 | 0.28204 | 0.00361 | 0.692 | -8.6 | -4.7 | 1734 | 23 | 1660 | 15 | 1602 | 18 |
| CLGC_0110_12 | 588 | 154.7 | 0.3 | 8230 | 0.12385 | 0.00263 | 4.33626 | 0.14864 | 0.25393 | 0.00683 | 0.785 | -30.7 | -25.9 | 2012 | 36 | 1700 | 28 | 1459 | 35 |
| CLGC_0110_14 | 289 | 76.3 | 1.7 | 991 | 0.10694 | 0.00165 | 4.58989 | 0.08894 | 0.30392 | 0.0036 | 0.601 | -1.4 | . | 1680 | 12 | 1747 | 27 | 1738 | 18 |
| CLGC_0110_14 | 289 | 76.3 | 1.7 | 991 | 0.10694 | 0.00165 | 3.833992 | 0.07404 | 0.26043 | 0.003 | 0.598 | -16.4 | -12.6 | 1748 | 27 | 1601 | 16 | 1492 | 15 |

Heavy font: Used in geochronological calculations.

Sample LSL-09-67. In this sample, 12 concordant zircons yield a concordia age of 1807 ± 10 Ma, which is considered as the crystallization age for the granite (Fig. 4d). The remaining 12 analyses are discordant along a poorly defined lead-loss line to a Phanerozoic lower intercept.

Sample LSL-09-68. This sample shows a distinctive concordant cluster ($n = 9$) at an early Paleoproterozoic age of 2118 ± 13 Ma, which is considered as the crystallization age for the granite, and evidence of inheritance of late Archean (2695 ± 13 Ma; Table 1, Fig. 3f) zircon (Fig. 4e). Discordant zircons in the sample scatter around a poorly defined lead-loss line to a Neoproterozoic or early Phanerozoic lower intercept.

5. Lu–Hf isotopes

Present-day $^{176}\text{Hf}/^{177}\text{Hf}$ in the zircons analyzed (Table 2) range from 0.28097 to 0.28148, at $^{176}\text{Lu}/^{177}\text{Hf} \leq 0.004$. $^{176}\text{Yb}/^{177}\text{Hf}$ ranges up to 0.2, but only 12 out of 108 single spot analyses show $^{176}\text{Yb}/^{177}\text{Hf}$ above 0.1, i.e. outside of the range of variation of the Temora-2 reference zircon ($^{176}\text{Yb}/^{177}\text{Hf} = 0.01$ to 0.11; Andersen et al., 2009). There is no correlation between $^{176}\text{Hf}/^{177}\text{Hf}$ at the time of crystallization and $^{176}\text{Yb}/^{177}\text{Hf}$ (Fig. 5a), suggesting that the empirical correction for interfering isotopes at mass 176 has not induced any bias in the results (e.g. Andersen et al. 2009; Heinonen et al. 2010). At the low $^{176}\text{Lu}/^{177}\text{Hf}$ observed for the zircons ($^{176}\text{Lu}/^{177}\text{Hf} = 0.0002$ to 0.004; Table 2), in-situ radiogenic growth can account for no more than ca. 20 % of the total observed variation in present-day $^{176}\text{Hf}/^{177}\text{Hf}$ (Fig. 5b), the remainder of which must be due to heterogeneous initial Hf isotope composition of the zircons.

In Fig. 6, time-corrected $^{176}\text{Hf}/^{177}\text{Hf}$ of the individual zircon is plotted against

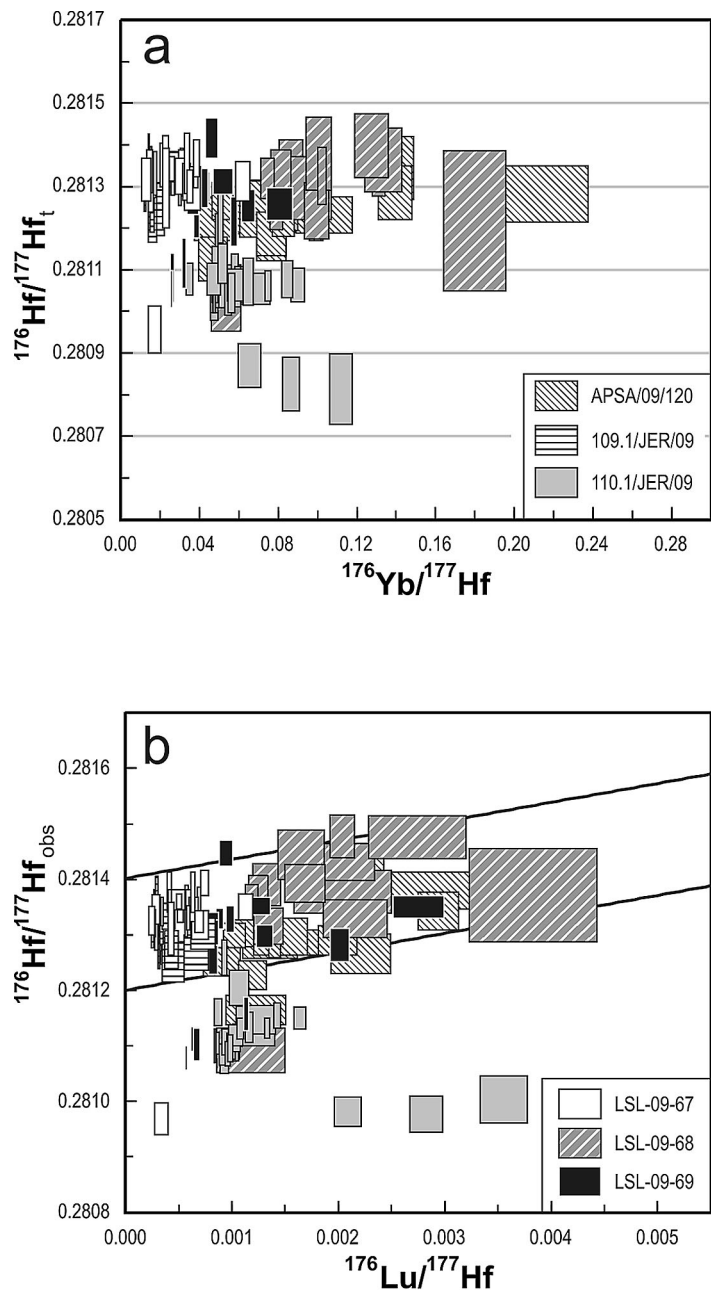


Fig. 5. (a) The relationship between $^{176}\text{Yb}/^{177}\text{Hf}$ and initial $^{176}\text{Hf}/^{177}\text{Hf}$. Data from Table 2. There is no residual correlation in this diagram, suggesting that the empirical correction for interference at mass 176 from ^{176}Yb has worked correctly (cf. Heinonen et al., 2010). Error boxes show $\pm 2\text{SE}_{\text{int}}$ for the individual analyses. (b) Present day $^{176}\text{Hf}/^{177}\text{Hf}$ plotted against $^{176}\text{Lu}/^{177}\text{Hf}$. The heavy lines are reference isochrons at an age of 1.8 Ga with initial $^{176}\text{Hf}/^{177}\text{Hf}$ of 0.2812 and 0.2814, respectively. Clearly, only part of the range of variation in initial $^{176}\text{Hf}/^{177}\text{Hf}$ can be accounted for by in-situ radiogenic accumulation. Error boxes show $\pm 2\text{SE}_{\text{int}}$ for the individual analyses.

Table 2 Lu-Hf isotope analyses and time-corrected parameters of zircon in granite and amphibolite from southern Lapland.

| Sample | Analysis | $^{176}\text{Hf}/^{177}\text{Hf}$ | 1σ | $^{176}\text{Lu}/^{177}\text{Hf}$ | 1σ | $^{176}\text{Yb}/^{177}\text{Hf}$ | 1σ | Age(Ga) | $^{176}\text{Hf}/^{177}\text{Hf}_t$ | 2σ | $\varepsilon\text{Hf}(t)$ | 2σ | t_{DM} | 2σ |
|--------------|---------------------|-----------------------------------|-----------|-----------------------------------|-----------|-----------------------------------|-----------|---------|-------------------------------------|-----------|---------------------------|-----------|-----------------|-----------|
| 109.1/JER/09 | JER109_10 | 0.281332 | 0.000012 | 0.00027 | 0.00001 | 0.013 | 0.000 | 1.79 | 0.28132 | 0.00002 | -11.4 | 0.8 | 2.60 | 0.02 |
| | JER109_11 | 0.281296 | 0.000012 | 0.00031 | 0.00001 | 0.015 | 0.000 | 1.81 | 0.28129 | 0.00002 | -12.3 | 0.8 | 2.65 | 0.02 |
| | JER109_12 | 0.281376 | 0.000015 | 0.00027 | 0.00001 | 0.013 | 0.000 | 1.79 | 0.28137 | 0.00003 | -9.8 | 1.1 | 2.55 | 0.02 |
| | JER109_13 | 0.281271 | 0.000015 | 0.00029 | 0.00000 | 0.014 | 0.000 | 1.80 | 0.28126 | 0.00003 | -13.5 | 1.1 | 2.69 | 0.02 |
| | JER109_14 | 0.281306 | 0.000014 | 0.00023 | 0.00000 | 0.011 | 0.000 | 1.79 | 0.28130 | 0.00003 | -12.3 | 1.0 | 2.64 | 0.02 |
| | JER109_15 | 0.281320 | 0.000011 | 0.00027 | 0.00001 | 0.013 | 0.000 | 1.79 | 0.28131 | 0.00002 | -11.8 | 0.8 | 2.62 | 0.01 |
| | JER109_24 | 0.281253 | 0.000018 | 0.00043 | 0.00005 | 0.015 | 0.001 | 1.78 | 0.28124 | 0.00004 | -14.6 | 1.2 | 2.72 | 0.02 |
| | JER109_25 | 0.281269 | 0.000016 | 0.00064 | 0.00006 | 0.019 | 0.001 | 1.78 | 0.28125 | 0.00003 | -14.3 | 1.0 | 2.71 | 0.02 |
| | JER109_27 | 0.281304 | 0.000010 | 0.00032 | 0.00001 | 0.015 | 0.000 | 1.78 | 0.28129 | 0.00002 | -12.6 | 0.7 | 2.64 | 0.01 |
| | JER109_29 | 0.281315 | 0.000015 | 0.00027 | 0.00000 | 0.014 | 0.000 | 1.78 | 0.28131 | 0.00003 | -12.2 | 1.1 | 2.63 | 0.02 |
| | JER109_34 | 0.281274 | 0.000017 | 0.00041 | 0.00003 | 0.015 | 0.001 | 1.78 | 0.28126 | 0.00003 | -13.8 | 1.1 | 2.69 | 0.02 |
| | JER109_36 | 0.281335 | 0.000012 | 0.00038 | 0.00003 | 0.015 | 0.001 | 1.78 | 0.28132 | 0.00002 | -11.7 | 0.8 | 2.61 | 0.01 |
| | JER109_42 | 0.281303 | 0.000014 | 0.00071 | 0.00006 | 0.022 | 0.001 | 1.78 | 0.28128 | 0.00003 | -13.1 | 0.9 | 2.67 | 0.01 |
| | JER109_43 | 0.281272 | 0.000012 | 0.00039 | 0.00004 | 0.017 | 0.001 | | | | | | | |
| 110.1/JER/09 | JER110_1-01c | 0.281074 | 0.000011 | 0.00091 | 0.00002 | 0.047 | 0.001 | 2.78 | 0.28103 | 0.00002 | 1.2 | 0.7 | 2.99 | 0.01 |
| | JER110_1-02c | 0.281093 | 0.000008 | 0.00098 | 0.00004 | 0.050 | 0.002 | 2.80 | 0.28104 | 0.00002 | 2.0 | 0.4 | 2.97 | 0.01 |
| | JER110_1-05c | 0.281121 | 0.000009 | 0.00123 | 0.00008 | 0.066 | 0.005 | | | | | | | |
| | JER110_1-05c_maxREE | 0.281151 | 0.000010 | 0.00163 | 0.00003 | 0.089 | 0.002 | 2.76 | 0.28107 | 0.00002 | 1.9 | 0.6 | 2.94 | 0.01 |
| | JER110_1-06c | 0.281085 | 0.000009 | 0.00091 | 0.00002 | 0.047 | 0.001 | | | | | | | |
| | JER110_1-06r | 0.280983 | 0.000013 | 0.00208 | 0.00006 | 0.064 | 0.003 | | | | | | | |
| | JER110_1-08r_all | 0.281206 | 0.000016 | 0.00105 | 0.00005 | 0.049 | 0.001 | 1.76 | 0.28117 | 0.00003 | -17.5 | 1.0 | 2.83 | 0.02 |
| | JER110_1-08r_end | 0.281148 | 0.000013 | 0.00126 | 0.00007 | 0.048 | 0.001 | 1.76 | 0.28111 | 0.00003 | -19.8 | 0.8 | 2.92 | 0.01 |
| | JER110_1-08r_front | 0.281260 | 0.000016 | 0.00091 | 0.00001 | 0.050 | 0.001 | 1.76 | 0.28123 | 0.00003 | -15.4 | 1.1 | 2.74 | 0.02 |
| | JER110_1-09c | 0.281108 | 0.000012 | 0.00092 | 0.00001 | 0.048 | 0.001 | 2.80 | 0.28106 | 0.00002 | 2.6 | 0.8 | 2.95 | 0.01 |
| | JER110_1-11c | 0.281095 | 0.000010 | 0.00102 | 0.00002 | 0.054 | 0.001 | 2.75 | 0.28104 | 0.00002 | 0.9 | 0.7 | 2.97 | 0.01 |
| | JER110_1-12c | 0.281106 | 0.000009 | 0.00097 | 0.00001 | 0.051 | 0.001 | 2.80 | 0.28105 | 0.00002 | 2.5 | 0.6 | 2.95 | 0.01 |
| | JER110_1-13c | 0.281096 | 0.000008 | 0.00097 | 0.00002 | 0.051 | 0.001 | 2.81 | 0.28104 | 0.00002 | 2.4 | 0.5 | 2.97 | 0.01 |
| | JER110_1-13r | 0.281344 | 0.000009 | 0.00067 | 0.00000 | 0.033 | 0.000 | 1.79 | 0.28132 | 0.00002 | -11.4 | 0.6 | 2.61 | 0.01 |
| | JER110_1-16c | 0.281113 | 0.000010 | 0.00064 | 0.00001 | 0.034 | 0.001 | | | | | | | |
| | JER110_1-17c2 | 0.281151 | 0.000011 | 0.00106 | 0.00002 | 0.057 | 0.001 | 2.76 | 0.28110 | 0.00002 | 3.1 | 0.7 | 2.90 | 0.01 |
| | JER110_1-18c | 0.281106 | 0.000010 | 0.00085 | 0.00001 | 0.047 | 0.001 | 2.73 | 0.28106 | 0.00002 | 1.3 | 0.6 | 2.94 | 0.01 |
| | JER110_1-19c | 0.281122 | 0.000011 | 0.00106 | 0.00001 | 0.061 | 0.001 | 2.77 | 0.28107 | 0.00002 | 2.3 | 0.8 | 2.94 | 0.01 |
| | JER110_1-20c | 0.281094 | 0.000009 | 0.00098 | 0.00002 | 0.054 | 0.001 | 2.83 | 0.28104 | 0.00002 | 2.8 | 0.5 | 2.97 | 0.01 |
| | JER110_1-20r | 0.280979 | 0.000016 | 0.00282 | 0.00008 | 0.086 | 0.002 | 2.80 | 0.28083 | 0.00003 | -5.4 | 0.8 | 3.28 | 0.02 |
| | JER110_21c | 0.281116 | 0.000012 | 0.00103 | 0.00002 | 0.059 | 0.001 | | | | | | | |

| Sample | Analysis | $^{176}\text{Hf} / ^{177}\text{Hf}$ | 1σ | $^{174}\text{Lu} / ^{177}\text{Hf}$ | 1σ | $^{176}\text{Yb} / ^{177}\text{Hf}$ | 1σ | Age(Ga) | $^{176}\text{Hf} / ^{177}\text{Hf}$ | 2σ | $\varepsilon\text{Hf(t)}$ | 2σ | t_{DM} | 2σ |
|--------------------|----------|-------------------------------------|-----------|-------------------------------------|-----------|-------------------------------------|-----------|---------|-------------------------------------|-----------|---------------------------|-----------|-----------------|-----------|
| JER110-24c | | 0.281087 | 0.000011 | 0.00095 | 0.00001 | 0.053 | 0.001 | 2.81 | 0.28104 | 0.00002 | 2.2 | 0.7 | 2.98 | 0.01 |
| JER110-28c_All | | 0.281120 | 0.000010 | 0.00102 | 0.00004 | 0.057 | 0.002 | 2.81 | 0.28106 | 0.00002 | 3.3 | 0.5 | 2.94 | 0.01 |
| JER110-28c_End | | 0.281135 | 0.000014 | 0.00114 | 0.00002 | 0.064 | 0.001 | 2.81 | 0.28107 | 0.00003 | 3.6 | 0.9 | 2.93 | 0.02 |
| JER110-28c_Front | | 0.281102 | 0.000015 | 0.00083 | 0.00001 | 0.046 | 0.000 | 2.81 | 0.28106 | 0.00003 | 3.0 | 1.0 | 2.95 | 0.02 |
| JER110-30c | | 0.281134 | 0.000009 | 0.00132 | 0.00001 | 0.074 | 0.001 | | | | | | | |
| JER110-62c | | 0.281132 | 0.000010 | 0.00106 | 0.00002 | 0.046 | 0.002 | 2.62 | 0.28108 | 0.00002 | -0.8 | 0.6 | 2.93 | 0.01 |
| JER110-63c | | 0.281156 | 0.000011 | 0.00141 | 0.00002 | 0.084 | 0.001 | 2.82 | 0.28108 | 0.00002 | 4.0 | 0.7 | 2.92 | 0.01 |
| JER110-64c | | 0.281097 | 0.000012 | 0.00097 | 0.00001 | 0.055 | 0.001 | 2.79 | 0.28105 | 0.00002 | 1.9 | 0.8 | 2.97 | 0.02 |
| JER110-64r | | 0.281005 | 0.000021 | 0.00355 | 0.00011 | 0.111 | 0.003 | | | | | | | |
| JER110-65c | | 0.281162 | 0.000012 | 0.00085 | 0.00002 | 0.050 | 0.001 | 2.78 | 0.28112 | 0.00002 | 4.3 | 0.8 | 2.87 | 0.01 |
| APSA-09-120 | | | | | | | | | | | | | | |
| APSA-01 | | 0.281280 | 0.000011 | 0.00134 | 0.000013 | 0.075 | 0.007 | 1.75 | 0.28124 | 0.00002 | -15.5 | 0.5 | 2.75 | 0.01 |
| APSA-02 | | 0.281264 | 0.000011 | 0.00097 | 0.00001 | 0.059 | 0.001 | 1.77 | 0.28123 | 0.00002 | -15.2 | 0.8 | 2.74 | 0.01 |
| APSA-03 | | 0.281253 | 0.000013 | 0.00089 | 0.00009 | 0.046 | 0.005 | 1.74 | 0.28122 | 0.00003 | -16.0 | 0.7 | 2.75 | 0.01 |
| APSA-04 | | 0.281381 | 0.000017 | 0.00295 | 0.00024 | 0.204 | 0.017 | 1.74 | 0.28128 | 0.00003 | -13.8 | 0.6 | 2.72 | 0.01 |
| APSA-05 | | 0.281287 | 0.000011 | 0.00162 | 0.00010 | 0.102 | 0.007 | 1.75 | 0.28123 | 0.00002 | -15.5 | 0.5 | 2.76 | 0.01 |
| APSA-06 | | 0.281165 | 0.000013 | 0.00121 | 0.00014 | 0.046 | 0.004 | 1.63 | 0.28113 | 0.00003 | -21.9 | 0.6 | 2.89 | 0.01 |
| APSA-07 | | 0.281425 | 0.000019 | 0.00237 | 0.00003 | 0.143 | 0.003 | | | | | | | |
| APSA-09 | | 0.281304 | 0.000012 | 0.00113 | 0.00006 | 0.070 | 0.003 | 1.67 | 0.28127 | 0.00002 | -16.1 | 0.7 | 2.70 | 0.01 |
| APSA-10 | | 0.281267 | 0.000018 | 0.00220 | 0.00014 | 0.076 | 0.004 | 1.73 | 0.28119 | 0.00004 | -17.3 | 1.0 | 2.83 | 0.01 |
| APSA-20 | | 0.281289 | 0.000012 | 0.00137 | 0.00009 | 0.082 | 0.004 | 1.74 | 0.28124 | 0.00002 | -15.3 | 0.6 | 2.74 | 0.01 |
| APSA-21 | | 0.281300 | 0.000011 | 0.00101 | 0.00005 | 0.051 | 0.003 | 1.77 | 0.28127 | 0.00002 | -13.8 | 0.7 | 2.70 | 0.01 |
| APSA-24 | | 0.281298 | 0.000017 | 0.00156 | 0.00007 | 0.069 | 0.005 | 1.70 | 0.28125 | 0.00003 | -16.1 | 1.1 | 2.74 | 0.02 |
| APSA-25 | | 0.281344 | 0.000017 | 0.00292 | 0.00010 | 0.178 | 0.004 | 1.76 | 0.28125 | 0.00003 | -14.8 | 1.0 | 2.77 | 0.02 |
| APSA-26 | | 0.281291 | 0.000013 | 0.00198 | 0.00009 | 0.098 | 0.002 | 1.76 | 0.28122 | 0.00003 | -15.5 | 0.7 | 2.78 | 0.01 |
| APSA-27 | | 0.281228 | 0.000013 | 0.00118 | 0.00007 | 0.076 | 0.004 | 1.77 | 0.28119 | 0.00003 | -16.6 | 0.8 | 2.81 | 0.01 |
| APSA-28 | | 0.281360 | 0.000016 | 0.00229 | 0.00006 | 0.139 | 0.004 | 1.69 | 0.28129 | 0.00003 | -15.0 | 1.0 | 2.70 | 0.02 |
| APSA-29 | | 0.281292 | 0.000016 | 0.00139 | 0.00003 | 0.082 | 0.003 | 1.71 | 0.28125 | 0.00003 | -15.9 | 1.1 | 2.73 | 0.02 |
| LSL-09-67 | | | | | | | | | | | | | | |
| LSL2009-67-01 | | 0.281297 | 0.000012 | 0.00027 | 0.00001 | 0.014 | 0.001 | 1.83 | 0.28129 | 0.00002 | -11.8 | 0.8 | 2.65 | 0.02 |
| LSL2009-67-02 | | 0.281367 | 0.000013 | 0.00038 | 0.00000 | 0.019 | 0.000 | | | | | | | |
| LSL2009-67-03 | | 0.281389 | 0.000012 | 0.00039 | 0.00001 | 0.022 | 0.001 | | | | | | | |
| LSL2009-67-04a | | 0.281359 | 0.000009 | 0.00057 | 0.00001 | 0.031 | 0.000 | 1.77 | 0.28134 | 0.00002 | -11.3 | 0.6 | 2.59 | 0.01 |
| LSL2009-67-04b | | 0.281366 | 0.000009 | 0.00046 | 0.00004 | 0.024 | 0.002 | 1.77 | 0.28135 | 0.00002 | -10.8 | 0.5 | 2.57 | 0.01 |
| LSL2009-67-05 | | 0.281319 | 0.000013 | 0.00068 | 0.00004 | 0.035 | 0.002 | 1.75 | 0.28130 | 0.00003 | -13.2 | 0.8 | 2.65 | 0.01 |
| LSL2009-67-06c | | 0.281343 | 0.000013 | 0.00032 | 0.00001 | 0.016 | 0.000 | | | | | | | |
| LSL2009-67-06r | | 0.281338 | 0.000010 | 0.00042 | 0.00001 | 0.022 | 0.001 | 1.77 | 0.28132 | 0.00002 | -11.9 | 0.7 | 2.61 | 0.01 |
| LSL2009-67-07 | | 0.281354 | 0.000008 | 0.00058 | 0.00001 | 0.029 | 0.000 | 1.87 | 0.28133 | 0.00002 | -9.2 | 0.5 | 2.59 | 0.01 |
| LSL2009-67-08 | | 0.281349 | 0.000013 | 0.00049 | 0.00001 | 0.025 | 0.000 | 1.79 | 0.28133 | 0.00003 | -11.2 | 0.9 | 2.60 | 0.02 |
| LSL2009-67-09 | | 0.280970 | 0.000014 | 0.00031 | 0.00003 | 0.016 | 0.002 | | | | | | | |

| | | | | | | | | | | | | | |
|-------------------|-----------|----------|----------|---------|-------|-------|---------|---------|---------|-------|------|------|------|
| LSL2009_67-10c | 0.281351 | 0.000111 | 0.00003 | 0.061 | 0.002 | 1.79 | 0.28131 | 0.00002 | -11.7 | 0.8 | 2.63 | 0.01 | |
| LSL2009_67-10r | 0.281364 | 0.00009 | 0.000050 | 0.026 | 0.001 | 1.79 | 0.28135 | 0.00002 | -10.6 | 0.5 | 2.58 | 0.01 | |
| LSL2009_67-11 | 0.281361 | 0.000011 | 0.00025 | 0.014 | 0.000 | 1.76 | 0.28135 | 0.00002 | -10.9 | 0.8 | 2.56 | 0.01 | |
| LSL2009_67-12 | 0.281347 | 0.000013 | 0.00026 | 0.014 | 0.001 | 1.78 | 0.28134 | 0.00003 | -11.0 | 0.9 | 2.58 | 0.02 | |
| LSL2009_67-13 | 0.281361 | 0.000007 | 0.00049 | 0.00001 | 0.025 | 0.01 | 0.28134 | 0.00001 | -10.5 | 0.5 | 2.58 | 0.01 | |
| LSL2009_67-14 | 0.281312 | 0.000024 | 0.00041 | 0.00001 | 0.022 | 0.01 | 0.00000 | 0.00000 | -10.5 | 0.5 | 2.58 | 0.01 | |
| LSL2009_67-14c | 0.281322 | 0.000012 | 0.00026 | 0.013 | 0.000 | 0.01 | 0.00000 | 0.00000 | -10.5 | 0.5 | 2.58 | 0.01 | |
| LSL2009_67-14r | 0.281326 | 0.000013 | 0.00023 | 0.012 | 0.001 | 1.79 | 0.28134 | 0.00002 | -10.7 | 0.8 | 2.59 | 0.01 | |
| LSL2009_67-15 | 0.281365 | 0.000011 | 0.00068 | 0.00001 | 0.037 | 0.01 | 0.00000 | 0.00000 | -11.7 | 0.8 | 2.58 | 0.01 | |
| LSL2009_67-17 | 0.281367 | 0.000011 | 0.00056 | 0.00001 | 0.030 | 0.000 | 1.74 | 0.28135 | 0.00002 | -9.4 | 0.7 | 2.55 | 0.01 |
| LSL2009_67-16 | 0.281394 | 0.000011 | 0.00072 | 0.00002 | 0.037 | 0.001 | 1.80 | 0.28137 | 0.00002 | -9.4 | 0.7 | 2.55 | 0.01 |
| LSL2009_67-18 | 0.281354 | 0.000014 | 0.00058 | 0.00001 | 0.030 | 0.001 | 1.77 | 0.28133 | 0.00003 | -11.4 | 1.0 | 2.59 | 0.02 |
| LSL2009_67-19 | 0.281322 | 0.000012 | 0.00055 | 0.00001 | 0.029 | 0.000 | 1.79 | 0.28130 | 0.00002 | -12.2 | 0.8 | 2.64 | 0.02 |
| LSL2009_67-21 | 0.281347 | 0.000011 | 0.00062 | 0.00002 | 0.030 | 0.002 | 1.79 | 0.28133 | 0.00002 | -11.2 | 0.7 | 2.61 | 0.01 |
| LSL2009_67-22 | 0.281332 | 0.000011 | 0.00057 | 0.00001 | 0.032 | 0.001 | 1.81 | 0.28131 | 0.00002 | -11.3 | 0.8 | 2.62 | 0.01 |
| LSL2009_67-23 | 0.281377 | 0.000018 | 0.00061 | 0.00001 | 0.033 | 0.001 | 1.80 | 0.28136 | 0.00004 | -10.1 | 1.3 | 2.57 | 0.02 |
| LSL2009_67-24 | 0.281324 | 0.000010 | 0.00068 | 0.00002 | 0.034 | 0.001 | 0.00000 | 0.00000 | -10.1 | 1.3 | 2.57 | 0.02 | |
| LSL-09-68 | | | | | | | | | | | | | |
| LSL0968-01 | 0.281373 | 0.000042 | 0.00382 | 0.00030 | 0.179 | 0.008 | 2.12 | 0.28122 | 0.00008 | -7.5 | 2.1 | 2.80 | 0.04 |
| LSL0968-03 | 0.281317 | 0.000016 | 0.00132 | 0.00007 | 0.078 | 0.002 | 2.15 | 0.28126 | 0.00003 | -5.3 | 0.9 | 2.70 | 0.02 |
| LSL0968-04 | 0.281391 | 0.000019 | 0.00131 | 0.00007 | 0.086 | 0.003 | 0.00000 | 0.00004 | -5.4 | 0.7 | 2.66 | 0.01 | |
| LSL0968-05 | 0.281378 | 0.000019 | 0.00203 | 0.00023 | 0.095 | 0.006 | 2.09 | 0.28130 | 0.00003 | -2.8 | 1.0 | 2.61 | 0.02 |
| LSL0968-07 | 0.281375 | 0.000016 | 0.00023 | 0.00005 | 0.081 | 0.003 | 2.16 | 0.28132 | 0.00003 | -6.5 | 0.8 | 2.74 | 0.01 |
| LSL0968-08 | 0.281330 | 0.000017 | 0.00214 | 0.00015 | 0.099 | 0.003 | 2.13 | 0.28124 | 0.00003 | -2.4 | 0.9 | 2.59 | 0.02 |
| LSL0968-09 | 0.281432 | 0.000017 | 0.00209 | 0.00012 | 0.130 | 0.002 | 2.14 | 0.28135 | 0.00003 | -2.4 | 0.9 | 2.59 | 0.02 |
| LSL0968-11 | 0.281476 | 0.000019 | 0.00274 | 0.00023 | 0.133 | 0.005 | 2.12 | 0.28137 | 0.00004 | -2.2 | 0.7 | 2.57 | 0.01 |
| LSL0968-12 | 0.281478 | 0.000019 | 0.00202 | 0.00006 | 0.127 | 0.004 | 2.04 | 0.28140 | 0.00004 | -2.9 | 1.2 | 2.52 | 0.02 |
| LSL0968-15 | 0.281445 | 0.000022 | 0.00164 | 0.00011 | 0.100 | 0.003 | 2.10 | 0.28138 | 0.00004 | -2.3 | 1.3 | 2.54 | 0.02 |
| LSL0968-20 | 0.281367 | 0.000012 | 0.00117 | 0.00003 | 0.074 | 0.002 | 2.12 | 0.28132 | 0.00002 | -3.9 | 0.8 | 2.62 | 0.01 |
| LSL0968-21c | 0.281093 | 0.000020 | 0.00116 | 0.00016 | 0.052 | 0.004 | 2.70 | 0.28103 | 0.00004 | -0.6 | 0.8 | 2.99 | 0.01 |
| LSL0968-22 | 0.281394 | 0.000017 | 0.00167 | 0.00010 | 0.102 | 0.001 | 2.12 | 0.28133 | 0.00003 | -3.7 | 0.9 | 2.61 | 0.02 |
| LSL-09-69 | | | | | | | | | | | | | |
| CLGC0110_01 | 0.281330 | 0.000009 | 0.00987 | 0.00002 | 0.043 | 0.000 | 1.78 | 0.28130 | 0.00002 | -12.5 | 0.6 | 2.65 | 0.01 |
| CLGC0110_02 | 0.281448 | 0.000012 | 0.0093 | 0.00003 | 0.045 | 0.002 | 1.72 | 0.28142 | 0.00002 | -9.5 | 0.8 | 2.49 | 0.01 |
| CLGC_0110_03 | 0.281299 | 0.000010 | 0.00129 | 0.00004 | 0.064 | 0.002 | 1.77 | 0.28126 | 0.00002 | -14.3 | 0.6 | 2.72 | 0.01 |
| CLGC_0110_04 | 0.281330 | 0.000012 | 0.0097 | 0.00002 | 0.042 | 0.001 | 1.77 | 0.28130 | 0.00002 | -12.8 | 0.8 | 2.65 | 0.01 |
| CLGC_0110_05 | 0.281320 | 0.000011 | 0.00980 | 0.00003 | 0.033 | 0.001 | 1.75 | 0.28129 | 0.00002 | -13.4 | 0.7 | 2.65 | 0.01 |
| CLGC_0110_06 | 0.281104 | 0.000015 | 0.00965 | 0.00002 | 0.025 | 0.001 | 1.78 | 0.28108 | 0.00003 | -20.2 | 1.0 | 2.93 | 0.02 |
| CLGC_0110_07 | 0.281256 | 0.000013 | 0.00981 | 0.00002 | 0.038 | 0.001 | 1.76 | 0.28123 | 0.00003 | -15.4 | 0.9 | 2.74 | 0.02 |
| CLGC_0110_08 | 0.281305 | 0.000011 | 0.00980 | 0.00003 | 0.036 | 0.002 | 1.77 | 0.28128 | 0.00002 | -13.5 | 0.7 | 2.67 | 0.01 |
| CLGC_0110_09 | 0.281080 | 0.000011 | 0.00955 | 0.00001 | 0.025 | 0.000 | 2.45 | 0.28105 | 0.00002 | -5.7 | 0.8 | 2.96 | 0.01 |
| CLGC_0110_12front | 0.281353 | 0.000008 | 0.00122 | 0.00007 | 0.051 | 0.003 | 1.68 | 0.28131 | 0.00002 | -14.2 | 0.4 | 2.64 | 0.01 |
| CLGC_0110_12 | 0.281159 | 0.000015 | 0.00111 | 0.00001 | 0.031 | 0.000 | 2.01 | 0.28112 | 0.00003 | -13.6 | 1.0 | 2.89 | 0.02 |
| CLGC_0110_13 | 0.281351 | 0.000010 | 0.00275 | 0.00012 | 0.080 | 0.003 | 1.76 | 0.28126 | 0.00002 | -14.3 | 0.4 | 2.75 | 0.01 |
| CLGC_0110_14 | 0.2811283 | 0.000015 | 0.00200 | 0.00005 | 0.057 | 0.001 | 1.75 | 0.28122 | 0.00003 | -16.1 | 1.0 | 2.79 | 0.02 |

the corresponding $^{207}\text{Pb}/^{206}\text{Pb}$ age. Zircons from the Archean sample 110.1/JER/09 generally plot above the CHUR curve and within the range of variation of zircon from the Pudasjärvi complex (Lauri et al., 2011). The exceptions are three analyses from rims of zoned grains plotting significantly below, at $\epsilon_{\text{Hf}} \leq -4$. Four zircons with $\epsilon_{\text{Hf}} \leq -11$ at 1.75–1.80 Ga are probably Archean grains that have lost lead in a Paleoproterozoic thermal event.

Most zircons from the Proterozoic samples plot within a field delimited by parallel Hf isotope growth lines starting from initial values of $\epsilon_{\text{Hf}} = +4$ and -8 at 2.7 Ga with slope corresponding to $^{176}\text{Lu}/^{177}\text{Hf} = 0.015$. This field overlaps with data for the late Archean Pudasjärvi complex, and represents the predicted total range of isotopic evolution lines for Hf by in-situ radiogenic growth in average late Archean crust of Pudasjärvi type (Lauri et al., 2011).

Since the slope of this trend is significantly less than that of the CHUR reservoir curve, ϵ_{Hf} will become significantly more negative with time. All of the zircons from the samples 109.1/JER/09 and LSL-09-68, as well as the majority of zircons from APSA-09-120, LSL-09-67 and LSL-09-69 fall within this main trend, and also overlap completely in Hf isotopes with the Nattanen-type granites of northern Finland (Fig. 6, data for Nattanen from Patchett et al., 1981). On the other hand, both the CLGC zircons and those from Nattanen have significantly less radiogenic Hf than the Revsund granite of northern Sweden (Fig. 6, data for Revsund from Vervoort & Patchett, 1996). The samples APSA-09-120, LSL-09-67 and LSL-09-69 have a few additional, less radiogenic zircons ($\epsilon_{\text{Hf}} < -15$). The ranges of variation in the samples 109.1/JER/09, APSA-09-120, LSL-09-67 and LSL-09-69 are

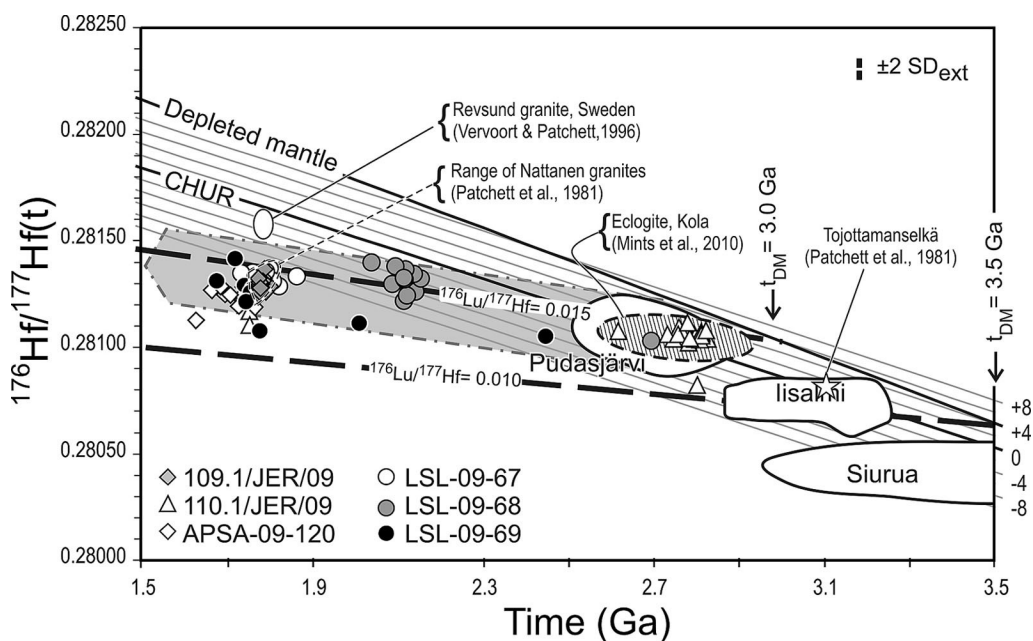


Fig. 6. Initial $^{176}\text{Hf}/^{177}\text{Hf}$ plotted at the $^{207}\text{Pb}/^{206}\text{Pb}$ age of the individual zircon, data from Table 1. Reference curves: CHUR: Bouvier et al. (2008); Depleted mantle: Griffin et al. (2000) modified by Andersen et al. (2009) to match the CHUR parameters used and a decay constant for ^{176}Lu of $1.867 \cdot 10^{-11}\text{a}^{-1}$. Thin lines parallel to the CHUR curve are constant ϵ_{Hf} contours drawn at 2 epsilon units interval, from $+8$ to -8 (scale in right margin of the diagram). The two heavy, broken lines are reference growth lines for crust with depleted mantle model age of 3.0 Ga and 3.5 Ga, corresponding to the average evolution with time of the main crustal reservoirs of the Neoarchaeon Pudasjärvi and the Mesoarchaeon lisalmi complexes, respectively (data from Lauri et al., 2011). The broad arrow outlined by a dash-dot line represents the overall expected variation with time due to in-situ radiogenic growth of ^{176}Hf in whole-rocks of the Pudasjärvi complex. Fields for zircons from the Pudasjärvi, lisalmi and Siurua complexes are from Lauri et al. (2011), Nattanen-type granites, northern Finland from Patchett et al. (1981) and Revsund granite, northern Sweden from Vervoort & Patchett (1996).

almost completely overlapping ($\epsilon_{\text{Hf}} = -10$ to -15 at 1.75–1.80 Ga). The main group of zircons in LSL-09-68 is slightly more radiogenic and plots towards the top of the main trend at $\epsilon_{\text{Hf}} = -2$ to -8 at ca. 2.1 Ga. One zircon from this sample is an inherited zircon plotting within the Pudasjärvi field. Two inherited zircons from the sample LSL-09-69 also plot within the main trend, but at early Paleoproterozoic ages.

6. Discussion

The evolution of the CLGC has been a largely unknown phase in the geological history of the Fennoscandian shield. The recognition of Archean rocks within the complex (see [Evins et al., 2002](#)) and age determinations of the Paleoproterozoic granites (see also [Lauerma, 1982](#); [Huhma, 1986](#); [Väänänen and Lehtonen, 2001](#); [Ahton et al., 2007](#)) along with Hf isotope data allow us to discuss the events that have affected the area since ca. 2.8 Ga.

The sample 110.1/JER/09 with an age of ca. 2.77 Ga represents the typical granodioritic to tonalitic gneiss of the Suomujärvi complex. [Evins et al. \(2002\)](#) describe this rock unit as “the 2810 Ma homogeneous Jumisko biotite tonalite–granodiorite” that commonly contains mafic inclusions, which [Evins et al. \(2002\)](#) also consider as Archean in age. Our results indicate that the main gneiss unit of the Suomujärvi complex is more heterogeneous than previously presumed. The zircon age obtained in this study for the amphibolite inclusions is Proterozoic, although an Archean crystallization age for the mafic protolith is fully possible, since the zircons are most probably metamorphic in origin. The Suomujärvi complex was affected by the Paleoproterozoic CLGC event, seen as the 1750–1800 Ma old zircons in both samples in this study and the 1.77–1.78 Ga monazite and titanite ages reported by [Corfu & Evins \(2002\)](#).

The ca. 2.1 Ga age of the granite sample LSL-09-68 is rare in the CLGC. Similar ages have been obtained for three other granitoid intrusions in the northern part of the CLGC ([Huhma, 1986](#); [Rastas](#)

[et al., 2001](#); [Ahton et al., 2007](#)), all of which are situated at the margin of the CLGC and the central Lapland greenstone belt, possibly forming a line of intrusions with approximately similar ages ([Fig. 7](#)). The central Lapland greenstone belt comprises volcanic and sedimentary formations ranging in age from ca. 2.4 Ga to <1.9 Ga (e.g., [Lehtonen et al., 1998](#); [Rastas et al., 2001](#); [Räsänen & Huhma, 2001](#)). Mafic magmatism with ages around 2.1 Ga is common in all of the Paleoproterozoic supracrustal belts of the northern Fennoscandian shield including the central Lapland greenstone belt (e.g., [Perttunen & Vaajoki, 2001](#); [Räsänen & Huhma, 2001](#)). The 2.1 Ga granites are markedly older than the majority of dated granites within the CLGC, which mostly show ages between 1.81 and 1.76 Ga ([Fig. 7](#)). It is possible that the 2.1 Ga old granite intrusions may belong to the evolution of the greenstone belt rather than to the CLGC and represent some kind of island arc or continental margin plutonism. Further age determinations and geochemistry are needed in order to test this hypothesis.

Our study area in the southern part of the CLGC hosts several granite types that were discussed by [Airo & Ahton \(1999\)](#). The older, ca. 1.81 Ga Pernu-type granites represented by sample LSL-09-67 are heterogeneous and migmatitic and commonly occur as sub-horizontal sheets that intrude their host rocks. The mode of occurrence resembles the granites of the southern Finland granite belt (see [Kurhila, 2011](#) and references therein), which were generated in a continental collision zone (e.g., [Kukkonen & Lauri, 2009](#)). The Pernu-type granites are found in the southwestern corner of the study area and they have not been found elsewhere within the CLGC, which may be due to limited amount of age data within the complex ([Fig. 7](#)). The younger, ca. 1.79 Ga old granites in the study area were grouped into the Jumisko-type by [Airo & Ahton \(1999\)](#), who described them as medium to coarse-grained, porphyritic, slightly deformed, red granites. The Jumisko-type granites are found northeast of the Pernu-type granites and the two types seem to be separated by the Ailanka fracture zone ([Airo, 1999](#)) in the central part of the study area ([Figs. 1](#)

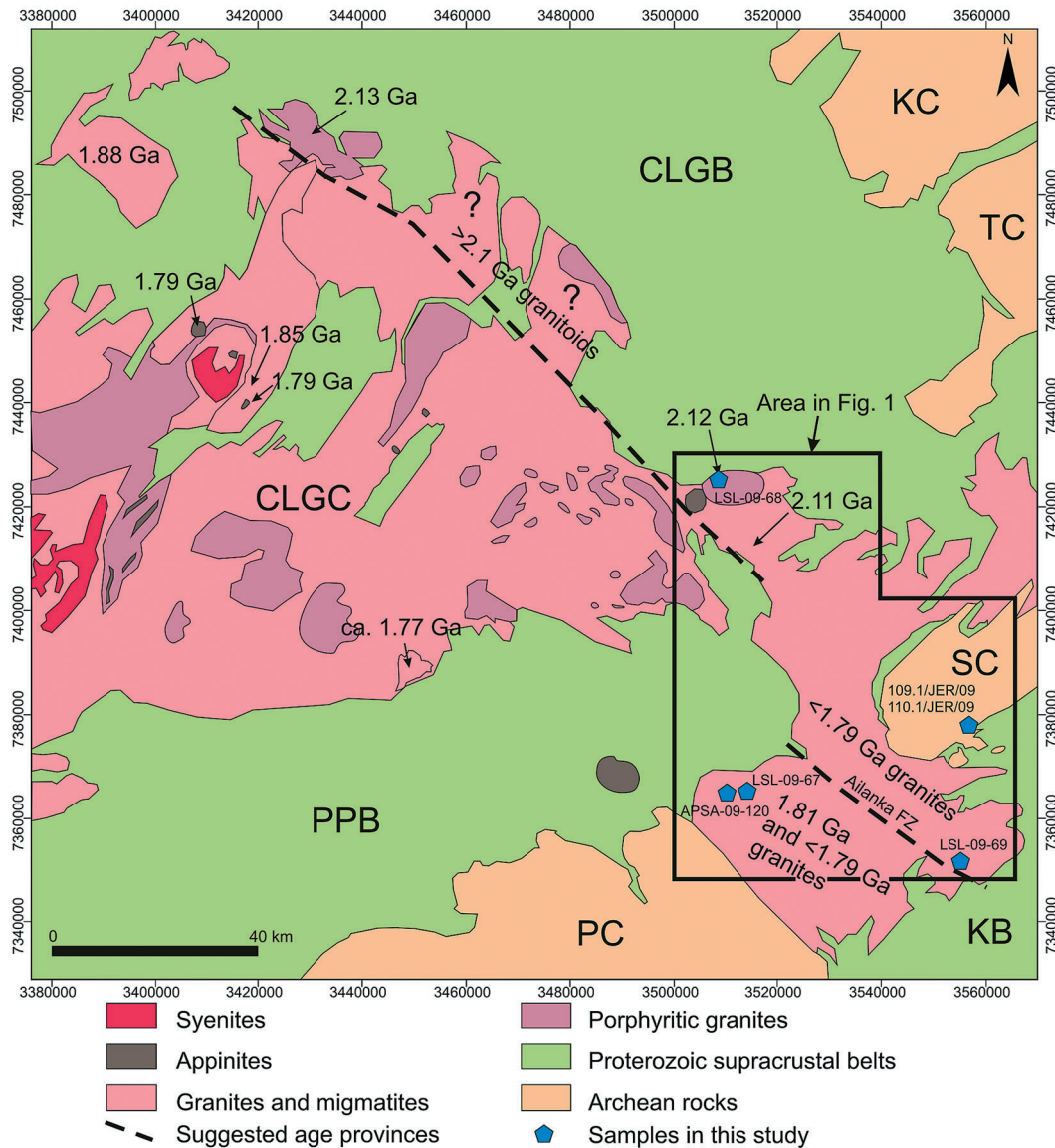


Fig. 7. Geological map of the Central Lapland granite complex with published age determinations (edited from the Digital Bedrock Map Database DigiKP, GTK). Dashed lines mark the boundaries of suggested age provinces for different granite types. Published ages are from Lauerma (1982), Huhma (1986), Rastas et al. (2001) and Ahtonen et al. (2007). CLGB = Central Lapland greenstone belt, CLGC = Central Lapland granitoid complex, KB = Kuusamo belt, KC = Koilliskaira complex, PC = Pudasjärvi complex, PPB = Peräpohja Belt, SC = Suomujärvi complex, TC = Tuntsa complex. Coordinates in KKJ.

& 7). Our sample set did not include samples of the Jumisko-type granites.

The samples APSA-09-120 and LSL-09-69 seem to represent a previously unrecognized granite type within the CLGC. The gray, fine-grained, non-foliated granite is found as small, irregular, dike-like plutons on both sides of the Ailanka fracture

zone. The age of this magmatic phase is 1.77–1.76 Ga, which is approximately similar to the post-orogenic Nattanen-type granites in northern Lapland (Haapala et al., 1987; Heilimo et al., 2009), and their zircons are similar in terms of initial Hf isotope composition (Fig. 6). However, the gray, fine-grained granite, which we call the Kellastentun-

turi-type, differs from the Nattanen-type granites both in the intrusion style and geochemistry (L.S. Lauri, *unpublished data*). The Nattanen-type plutons are geochemically I-type to A-type, large, concentric, multiphase stocks that cross-cut their wall rocks sharply and have intruded along crustal-scale faults (Haapala et al., 1987; Heilimo et al., 2009). The

Kellastentunturi-type granites seem to be composed of small volumes of locally generated granitic melts that have intruded local structures and most probably represent the last, post-kinematic phase in the magmatic evolution of southern CLGC.

Granitic and alkaline magmatism with ages around 1.8 Ga is widespread within the Fennoscandian shield. The 1.85–1.79 Ga late Svecofennian leucogranites of southern Finland were generated in the collisional zone between Fennoscandia and Sarmatia (e.g., Kukkonen & Lauri, 2009; Kurhila, 2011). Southern Finland also hosts post-orogenic alkaline syenites, lamprophyres and carbonatites that have ages between 1.80 Ga and 1.77 Ga (Eklund et al., 1998; Eklund & Shebanov, 2005). The situation in which both orogenic and post-orogenic rocks show approximately similar ages is common in both southern and northern Finland (see Ahtonen et al., 2007). However, in southern Finland the post-orogenic rocks with alkaline affinity are clearly the last phase in the magmatic succession whereas in Lapland the 1.79 Ga alkaline, appinitic intrusions (Väänänen, 2004; Ahtonen et al., 2007) have intruded in the middle of an orogenic granite event that continued for several tens of millions years after the emplacement of appinites. It thus seems that the nearly coeval granite magmatism in southern and northern Finland comprises two separate events in different tectonic settings.

All samples analyzed in this study show initial Hf isotope signatures compatible with an origin from Archean crust similar to that of the Pudasjärvi complex (Lauri et al. 2011), and with insignificant contributions from mantle-derived material. However, there are some differences that suggest subtle variation in source composition: Zircon in the sample LSL-09-68 (ca. 2.1 Ga) is marginally more radiogenic than that in the other samples,

suggesting either a younger crustal source, or a stronger, but still minor influence of mantle-derived material. There is no evidence of influence from crustal sources similar to the ca. 3.1–3.2 Ga Iisalmi and Tojottamanselkä complexes (Patchett et al., 1981; Lauri et al., 2011) in any of the rocks analyzed for this study (Fig. 6).

Evins et al. (2002) interpreted the Suomujärvi complex to be a part of the Belomorian province based on both magmatic and metamorphic ages of the complex (see also Corfu and Evins, 2002). Few Hf isotope data have been published from the Belomorian province, but the late Archean eclogites analysed by Mints et al. (2010) show complete overlap with both the present data from the Suomujärvi complex and previously published data from the Pudasjärvi complex (Lauri et al., 2011; Fig. 6). Hf isotope data thus can neither confirm nor reject the hypothesis by Evins et al. (2002) and Corfu & Evins (2002) that the Suomujärvi complex is associated to Belomoria rather than Karelia.

The westwards continuation of Neoarchean crust of the type that has given rise to the CLGC granitoids is not constrained by Hf isotope data due to lack of analyses. However, whole-rock Sm–Nd data on Paleoproterozoic granites suggest the existence of unexposed crustal rocks of Neoarchean age in the central part of the CLGC (Huhma, 1986; Ahtonen et al., 2007), in the Luleå–Jokkmokk area of northern Sweden, ca. 250 km south of the exposed Archean-Proterozoic boundary (Mellqvist et al., 1999), and possibly all the way to the Lofoten archipelago of northern Norway (Wade, 1985).

7. Conclusions

The border zone of Archean and Proterozoic rocks at southern Finnish Lapland shows over one billion years of geological history with granitoid-forming events at ca. 2.8 Ga, 2.12 Ga, 1.81 Ga and 1.76 Ga. The first magmatic event mainly formed granodiorites and tonalites of the Archean Suomujärvi complex whereas the next three events were characterized by granitic rocks. Mafic rocks are found mainly within the Archean Suomujärvi complex, but their age remains unresolved. The

granitic rocks have been included in the ca. 1.8 Ga central Lapland granitoid complex, which is more heterogeneous in terms of age than previously indicated. The 2.12 Ga granites are found at the margin of the central Lapland greenstone belt in the northern part of the study area and could be related to its tectonic evolution. The 1.81 Ga Pernu-type granites seem to be limited to the Archean Pudasjärvi complex on the SW side of the Ailanka fracture zone. The 1.76 Ga Kellastentunturi-type granites are found throughout the study area. All Proterozoic granites in the study area show isotopic evidence of a Neoarchean source that can be traced throughout the central Lapland granitoid complex to the Jokkmokk area in Sweden and possibly to the Lofoten area in Norway.

Acknowledgments

This study was done as a part of the GTK project 2511001 (Bedrock mapping of the Kemijärvi area). Students Aleksi Salo and Janne Kinnunen are acknowledged for their contribution to the geological mapping of the study area. Assistants Pauli Vuojärvi and Pertti Telkkälä took the age determination samples. Hans Kristian Daviknes and Siri Simonsen at the University of Oslo are thanked for sample processing and technical assistance with the LA-ICP-MS analyses. Prof. Olav Eklund and Dr. Jussi Heinonen are thanked for constructive reviews and Dr. Arto Luttinen is acknowledged for editorial comments that considerably improved the manuscript. This is contribution no. 25 from the Department of Geosciences, University of Oslo Isotope Geology Laboratory.

References

- Ahtonen, N., Hölttä, P. & Huhma, H. 2007. Intracratonic Palaeoproterozoic granitoids in northern Finland: prolonged and episodic crustal melting events revealed by Nd isotopes and U-Pb ages on zircon. *Bulletin of the Geological Society of Finland* 79, 143–174.
- Airo, M.-L. 1999. Aeromagnetic and petrophysical investigations applied to tectonic analysis in the northern Fennoscandian Shield. *Geological Survey of Finland, Report of Investigation* 145, 1–51.
- Airo, M.-L. & Ahtonen, N. 1999. Three different types of Svecokarelian granitoids in southeastern Lapland: Magnetic properties correlated with mineralogy. In: Autio, S. (Ed.), *Geological Survey of Finland, Current Research 1997–1998*, 129–140.
- Andersen, T., Andersson, U.B., Graham, S., Åberg, G. & Siemonsen, S.L. 2009. Granitic magmatism by melting of juvenile continental crust: New constraints on the source of Paleoproterozoic granitoids in Fennoscandia from Hf isotopes in zircon. *Journal of the Geological Society, London* 166, 233–248.
- Bedrock Map Database DigiKP Finland, GTK. Version 1.0, 04.08.2009. Extracted on March 26th, 2010.
- Bouvier, A., Vervoort, J.D. & Patchett, P.J. 2008. The Lu-Hf and Sm-Nd isotopic composition of CHUR: Constraints from unequilibrated chondrites and implications for the bulk composition of terrestrial planets. *Earth and Planetary Science Letters* 273, 48–57.
- Corfu, F. & Evans, P.M. 2002. Late Palaeoproterozoic monazite and titanite U–Pb ages in the Archean Suomujärvi Complex, N-Finland. *Precambrian Research* 116, 171–181.
- Corfu, F., Hanchar, J.M., Hoskin, P.W.O. & Kinny, P.D. 2003. Atlas of zircon textures. *Reviews in Mineralogy and Geochemistry* 53, 469–500.
- Eklund, O. & Shebanov, A. 2005. Prolonged postcollisional shoshonitic magmatism in the southern Svecofennian domain – a case study of the Åva granite–lamprophyre ring complex. *Lithos* 80, 229–247.
- Eklund, O., Konopelko, D., Rutanen, H., Fröjdö, S. & Shebanov, A.D., 1998. 1.8 Ga Svecofennian post-collisional shoshonitic magmatism in the Fennoscandian Shield. *Lithos* 45, 87–108.
- Evins, P.M., Mansfeld, J. & Laajoki, K. 2002. Geology and Geochronology of the Suomujärvi Complex: a new Archean gneiss region in the NE Baltic Shield, Finland. *Precambrian Research* 116, 285–306.
- Griffin, W.L., Pearson, N.J., Belousova, E., Jackson, S.E., van Achterbergh, E., O'Reilly, S.Y. & Shee, S.R. 2000. The Hf isotope composition of cratonic mantle: LAM-MC-ICPMS analysis of zircon megacrysts in kimberlites. *Geochimica et Cosmochimica Acta* 64, 133–147.
- Haapala, I., Front, K., Rantala, E. & Vaarma, M. 1987. Petrology of Nattanen-type granite complexes, northern Finland. *Precambrian Research* 35, 225–240.
- Hawkesworth, C.J. & Kemp, A.I.S. 2006. Using hafnium and oxygen isotopes in zircons to unravel the record of crustal evolution. *Chemical Geology* 226, 144–162.
- Heilimo, E., Halla, J., Lauri, L.S., Rämö, O.T., Huhma, H., Kurhila, M.I. & Front, K. 2009. The Paleoproterozoic Nattanen-type granites in northern Finland and vicinity – a postcollisional oxidized A-type suite. *Bulletin of the Geological Society of Finland* 81, 7–38.
- Heinonen, A.P., Andersen, T. & Rämö, O.T. 2010. Re-evaluation of rapakivi petrogenesis: Source constraints from the Hf isotope composition of zircon in the rapakivi granites and associated mafic rocks of southern Finland. *Journal of Petrology* 51, 1687–1709.
- Huhma, H. 1986. Sm-Nd, U-Pb and Pb-Pb isotopic evidence for the origin of the Early Proterozoic Svecokarelian crust

- in Finland. Geological Survey of Finland, Bulletin 337, 1–48.
- Jackson, S.E., Pearson, N.J., Griffin, W.L. & Belousova, E.A. 2004. The application of laser ablation-inductively coupled plasma-mass spectrometry (LA-ICP-MS) to in situ U-Pb zircon geochronology. *Chemical Geology* 211, 47–69.
- Kukkonen, I.T. & Lauri, L.S. 2009. Modelling the thermal evolution of a collisional Precambrian orogen: high heat production migmatitic granites of southern Finland. *Precambrian Research* 168(3–4), 233–246.
- Kurhila, M. 2011. Late Svecofennian leucogranites of southern Finland – chronicles of an orogenic collapse. Ph.D. Thesis, Department of Geosciences and Geography A8, University of Helsinki, Finland, 23 p.
- Lauerma, R. 1982. On the ages of some granitoid and schist complexes in northern Finland. *Bulletin of the Geological Society of Finland* 54, 85–100.
- Lauri, L.S., Andersen, T., Hölttä, P., Huhma, H. & Graham, S. 2011. Evolution of the Archaean Karelian province in the Fennoscandian Shield in the light of U-Pb zircon ages and Sm-Nd and Lu-Hf isotope systematics. *Journal of the Geological Society, London* 168, 201–218.
- Lehtonen, M.I., Airo, M-L., Eilu, P., Hanski, E., Kortelainen, V., Lanne, E., Manninen, T., Rastas, P., Räsänen, J. & Virransalo, P. 1998. *Kittilän vihreäkivialueen geologia – Lapin vulkaniiittiprojektiin raportti*. Summary: The stratigraphy, petrology and geochemistry of the Kittilä greenstone area, northern Finland – a report of the Lapland Volcanite Project. Geological Survey of Finland, Report of Investigation 140, 1–144.
- Ludwig, K.R. 2003. User's Manual for Isoplot/Excel 3.00. A Geochronological Toolkit for Microsoft Excel. Berkeley Geochronology Center Special Publications 4, 1–70.
- Mellqvist, C., Öhlander, B., Skiöld, T. & Wikström, A. 1999. The Archaean-Proterozoic Paleoboundary in the Luleå area, northern Sweden: field and isotope geochemical evidence for a sharp terrane boundary. *Precambrian Research* 96, 225–243.
- Mints, M.V., Belousova, E.A., Konilov, A.N., Natapov, L.M., Shchipansky, A.A., Griffin, W.L., O'Reilly, S.Y., Dokukina, K.A. & Kaulina, T.V. 2010. Mesoarchean subduction processes: 2.87 Ga eclogites from the Kola Peninsula, Russia. *Geology* 38, 739–742.
- Patchett, P.J., Kouvo, O., Hedge, C.E. & Tatsumoto, M. 1981. Evolution of continental crust and mantle heterogeneity; evidence from Hf isotopes. *Contributions to Mineralogy and Petrology* 78, 279–297.
- Patison, N.L., Korja, A., Lahtinen, R., Ojala, V.J. & FIRE Working Group 2006. FIRE seismic reflection profiles 4, 4A and 4B: insights into the crustal structure of northern Finland from Ranua to Näätämö. In: Kukkonen, I.T. & Lahtinen, R. (Eds.) *Finnish Reflection Experiment FIRE 2001–2005*. Geological Survey of Finland, Special Paper 43, 161–222.
- Perttunen, V. & Vaajoki, M. 2001. U-Pb geochronology of the Peräpohja Schist Belt, northwestern Finland. In: Vaajoki, M. (Ed.) *Radiometric age determinations from Finnish Lapland and their bearing on the timing of Precambrian volcano-sedimentary sequences*. Geological Survey of Finland, Special Paper 33, 45–84.
- Räsänen, J. & Huhma, H. 2001. U-Pb datings in the Sodankylä schist area, central Finnish Lapland. In: Vaajoki, M. (Ed.) *Radiometric age determinations from Finnish Lapland and their bearing on the timing of Precambrian volcano-sedimentary sequences*. Geological Survey of Finland, Special Paper 33, 153–188.
- Rastas, P., Huhma, H., Hanski, E., Lehtonen, M.I., Härkönen, I., Kortelainen, V., Mänttäri, I. & Paakkola, J. 2001. U-Pb isotopic studies on the Kitilä greenstone area, central Lapland, Finland. In: Vaajoki, M. (Ed.) *Radiometric age determinations from Finnish Lapland and their bearing on the timing of Precambrian volcano-sedimentary sequences*. Geological Survey of Finland, Special Paper 33, 95–142.
- Rosa, D. R. N., Finch, A. A., Andersen, T. & Inverno, C. M. C. 2009. U-Pb geochronology and Hf isotope ratios of magmatic zircons from the Iberian Pyrite Belt. *Mineralogy and Petrology*, 95, 47–69.
- Söderlund, U., Patchett, P.J., Vervoort, J. & Isachsen, C.E. 2004. The ^{176}Lu decay constant determined by Lu-Hf and U-Pb isotope systematics of Precambrian mafic intrusions. *Earth and Planetary Science Letters* 219, 311–324.
- Väänänen, J. 2004. Sieppijärven ja Pasmajärven kartta-alueiden kallioperä. Summary: Pre-Quaternary rocks of the Sieppijärvi and Pasmajärvi map-sheet areas. Geological map of Finland 1:100 000, Explanation to the maps of Pre-Quaternary rocks, Sheets 2634 and 2642. Geological Survey of Finland, Espoo, 55 p.
- Väänänen, J. & Lehtonen, M.I. 2001. U-Pb isotopic age determinations from the Kolari-Muonio area, western Finnish Lapland. In: Vaajoki, M. (Ed.), *Radiometric age determinations from Finnish Lapland and their bearing on the timing of Precambrian volcano-sedimentary sequences*. Geological Survey of Finland, Special Paper 33, 85–93.
- Vervoort, J.D. & Patchett, P.J. 1996. Behaviour of hafnium and neodymium isotopes in the crust: Constraints from Precambrian crustally derived granites. *Geochimica et Cosmochimica Acta* 60, 3717–3733.
- Wade, S.J.R. 1985. Radiogenic isotope studies of crust-forming processes in the Lofoten-Vesterålen province of north Norway. Ph.D. Thesis, University of Oxford, UK.
- Wiedenbeck, M., Allé, P., Corfu, F., Griffin, W.L., Meier, M., Oberli, F., Von Quadt, A., Roddick, J.C. & Spiegel, W. 1995. Three natural zircon standards for U-Th-Pb, Lu-Hf, trace element and REE analysis. *Geostandards Newsletter* 19, 1–23.
- Woodhead, J.D. & Hergt, J.M. 2005. A preliminary appraisal

of seven natural zircon reference materials for in situ Hf isotope determination. *Geostandards and Geoanalytical Research* 29, 183–195.